# Vibrational Spectroscopy of the Ammoniated Ammonium Ions NH+ 4(NH3)n ( n = 1−10)

**ARTICLE** *in* THE JOURNAL OF PHYSICAL CHEMISTRY · MARCH 1991

Impact Factor: 2.78 · DOI: 10.1021/j100159a020



**3 AUTHORS**, INCLUDING:

Mark Crofton
Aerospace Corporation
**93** PUBLICATIONS **1,183** CITATIONS
SEE PROFILE

Yuan T. Lee
University of California, Berkeley
**226** PUBLICATIONS **6,672** CITATIONS
SEE PROFILE

# Vibrational Spectroscopy of the Ammoniated Ammonium Ions $NH_4^+(NH_3)_n$ ($n$ = 1-10)

J. M. Price, M. W. Crofton, and Y. T. Lee*

*Materials and Chemical Sciences Division, Lawrence Berkeley Laboratory and Department of Chemistry, University of California, Berkeley, California 94720* *(Received: May 17, 1990)*

The gas-phase vibration-internal rotation spectra of mass-selected ammoniated ammonium ions, $NH_4^+(NH_3)_n$ (for $n$ = 1-10), have been observed from 2600 to 4000 $cm^{-1}$. The spectra show vibrational features that have been assigned to modes involving both the ion core species, $NH_4^+$, and the first shell $NH_3$ solvent molecules. Nearly free internal rotation of the solvent molecules about their local $C_3$ axes in the first solvation shell has been observed in the smaller clusters ($n$ = 1-6). For the largest clusters studied ($n$ = 7-10) the spectra converge, with little difference between clusters differing by one solvent molecule. For these clusters, the spectrum in the 3200-3500 $cm^{-1}$ region is quite similar to that of liquid ammonia, and the entire region of 2600-3500 $cm^{-1}$ also bears considerable resemblance to the spectra of ammonium salts dissolved in liquid ammonia under some chemical conditions. This indicates the onset of a liquidlike environment for the ion core and first shell solvent molecules in clusters as small as $NH_4^+(NH_3)_8$.

## Introduction

Early spectroscopic studies of the ammonium ion were confined to the condensed phases and employed direct IR absorption measurements of either crystals of ammonium salts or ammonium salts dissolved in solution.[1-3] These measurements revealed spectral features that were assigned to vibrational modes of the perturbed $NH_4^+$ ion ($T_d$ symmetry). Of these, the strongest in the 2000-4000-$cm^{-1}$ region were found to involve the triply degenerate antisymmetric stretching motion $\nu_3$ and the first overtone of the doubly degenerate bending motion $2\nu_4$ (see Figure 1).

Gas-phase studies which followed centered for the most part on the thermodynamics and kinetics of clustering reactions at relatively high pressures. Many investigators contributed in the effort to determine the $\Delta H°$ for formation of the solvated ammonium ion $NH_4^+(NH_3)_n$.[4-10] Kebarle and co-workers showed that in the larger clusters there was a discontinuity in the $\Delta H°$ for the $n = 4 \rightarrow n = 5$ clustering step. This result was consistent with the idea that there were four solvent molecules involved in the first solvation shell of the cluster, with the solvent ammonias probably oriented along the N-H bonds of the ammonium ion due to ion-dipole interaction. A summary of these results appears in Table I, which lists the $\Delta H°$ of formation for each clustering step in the $NH_4^+(NH_3)_n + NH_3 \rightleftarrows NH_4^+(NH_3)_{n+1}$ reaction series.

A fairly extensive body of theoretical work also exists, investigating the structure and thermodynamics of these systems. Pullman and Armbruster examined the thermodynamics of the stepwise addition of $H_2O$ or $NH_3$ to $NH_4^+$ for one to five solvent molecules and managed to reproduce the qualitative features of the experimental data.[11] The experimental change in preferential addition from $NH_3$ at low levels of solvation to $H_2O$ at higher levels of solvation was reproduced. Errors in the energies calculated from the STO 3G basis set were found to decrease with increasing number of solvent molecules.

A more recent series of calculations on the thermodynamics of the $NH_4^+(NH_3)_n$ ($n$ = 1-5) ions as well as their detailed structures have been made by Hirao et al.[12] In this work, ab initio molecular orbital calculations determined the structure and binding energies of the series in reasonable agreement with high-pressure equilibrium measurements. Values for the solvation energies obtained from this work, using 3-21G, 3-21G*, and 6-31G** basis sets, yielded consistently higher values than experimentally obtained.

Gas-phase spectroscopic measurements for the ammonium ion and the ammoniated ammonium clusters have only recently been carried out. The development of velocity modulation spectroscopy has yielded a great deal of information for a wide range of molecular ions, including the $NH_4^+$ ion.[13] The $\nu_3$ band of the ammonium ion has been investigated at high resolution by both Crofton and Oka[14] and Schafer and Saykally[15] using this tech-

**TABLE I: Thermodynamic Data (in kcal/mol) for Gas-Phase Clustering Reactions $NH_4^+(NH_3)_n + NH_3 \rightleftarrows NH_4^+(NH_3)_{n+1}$**

| $n$, | $n+1$ | $\Delta G°_{298}$[a] | $\Delta H°_{298}$[a] | $\Delta H°_{298}$[b] | $\Delta H°_{298}$[c] | $\Delta H°_0$[d] |
|---|---|---|---|---|---|---|
| 0, | 1 | -17.5 | -27 | -25.4 | -21.5 | -13.8 |
| 1, | 2 | | -17 | -17.3 | -16.2 | -6.4 |
| 2, | 3 | -6.4 | -16.5 | -17.3 | -13.5 | |
| 3, | 4 | -3.8 | -14.5 | -14.2 | -11.7 | |
| 4, | 5 | -0.2 | -7.5 | -11.8 | -7.0 | |

[a] Searles, S. K.; Kebarle, P. *J. Phys. Chem.* **1968**, *72*, 742. [b] Tang, I. N.; Castleman, Jr., A. W. *J. Chem. Phys.* **1972**, *62*, 4576. [c] Arshadi, M. R.; Futrell, J. H. *J. Phys. Chem.* **1974**, *78*, 1482. [d] Ceyer, S. T.; Tiedemann, P. W.; Mahan, B. H.; Lee, Y. T. *J. Chem. Phys.* **1979**, *70*, 14.

**TABLE II: Molecular Constants[a] for $NH_4^+$ and $NH_3$**

| $NH_4^+$ ($T_d$ Symmetry) | $NH_3$ ($C_{3v}$ Symmetry) |
|---|---|
| $\nu_1$: 3270 ± 25[b] | $\nu_1$: 3336.21[c] |
| $\nu_2$: 1669[d] | $\nu_2$: 950[e] |
| $\nu_3$: 3343.28[f] | $\nu_3$: 3444[e] |
| $\nu_4$: 1447.22[g] | $\nu_4$: 1627,[e] $2\nu_4^0$: 3216.71[c] |
| $A = B = C$: 5.9293 ± 0.0002[f] | $2\nu^4$: 3240.45[c] |
| $\zeta_3$: 0.0604[f] | $B = C$: 9.941,[h] $A$: 6.30$_9$[h] |
| | $\zeta_3$: 0.06[h] |

[a] Units are $cm^{-1}$ for all constants except $\zeta_3$, which is dimensionless. [b] Botschwina, P. *J. Chem. Phys.* **1987**, *87*, 1453; scaled ab initio value. [c] Benedict, W. S.; Plyler, E. K.; Tidwell, E. D. *J. Chem. Phys.* **1960**, *32*, 32. [d] DeFrees, D. J.; McLean, A. D. *J. Chem. Phys.* **1985**, *82*, 333; scaled ab initio value. [e] Shimanouchi, T. *Tables of Molecular Vibrational Frequencies*; Natl. Stand. Ref. Data Ser., Natl. Bur. Stand. No 39; U.S. Government Printing Office: Washington, DC, 1972. [f] Reference 14. [g] Polak, M.; Gruebele, M.; DeKock, B. W.; Saykally, R. J. *Mol. Phys.* **1989**, *66*, 1193. [h] See ref 38, p 437.

(1) Wagner, E. L.; Horning, D. F. *J. Chem. Phys.* **1949**, *18*, 296.
(2) Mathieu, J. P.; Poulet, H. *Spectrochim. Acta A* **1960**, *16*, 696.
(3) Corset, J.; Huong, P. V.; Lascombe, J. *Spectrochim. Acta A* **1968**, *24*, 2045.
(4) Hogg, A. M.; Kebarle, P. *J. Chem. Phys.* **1965**, *43*, 449.
(5) Hogg, A. M.; Haynes, R. M.; Kebarle, P. *J. Am. Chem. Soc.* **1966**, *88*, 28.
(6) Searles, S. K.; Kebarle, P. *J. Phys. Chem.* **1968**, *72*, 742.
(7) Payzant, J. D.; Cunningham, A. J.; Kebarle, P. *Can. J. Chem.* **1973**, *51*, 3242.
(8) Tang, I. N.; Castleman Jr., A. W. *J. Chem. Phys.* **1975**, *62*, 4576.
(9) Arshadi, M. R.; Futrell, J. H. *J. Phys. Chem.* **1974**, *78*, 1482.
(10) Ceyer, S. T.; Tiedemann, P. W.; Mahan, B. H.; Lee, Y. T. *J. Chem. Phys.* **1979**, *70* (1), 14.
(11) Pulman, A.; Armbuster, A. M. *Chem. Phys. Lett.* **1975**, *36*, 558.
(12) Hirao, K.; Fugikawa, T.; Konishi, H.; Yamabe, S. *Chem. Phys. Lett.* **1984**, *104*, 184.
(13) Gudeman, C. S.; Saykally, R. J. *Annu. Rev. Phys. Chem.* **1984**, *35*, 387.

0022-3654/91/2095-2182$02.50/0 

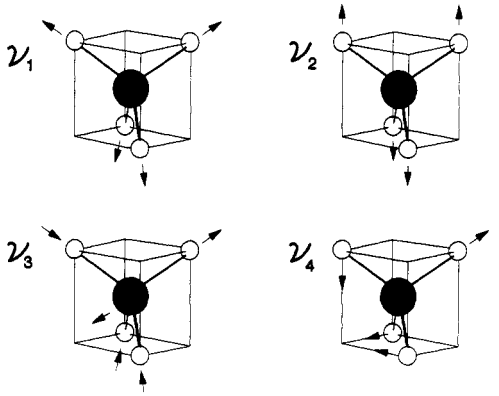


**Figure 1.** Normal vibrations of tetrahedrally symmetric $NH_4^+$. $\nu_3$ and $\nu_4$ are 3-fold degenerate, while $\nu_1$ and $\nu_2$ are 1- and 2-fold degenerate, respectively. Arrows in the figure indicate the direction of motion but are not to scale with the amplitudes. (See ref 38.)

nique. From these data on accurate equilibrium geometry has been obtained.[14] Table II lists the measured rotational constants and equilibrium geometry parameters for this ion and the $NH_3$ molecule. The only measurements of the spectra of the ammoniated ammonium ions ($n$ = 1–4) have been limited to the direct absorption measurements performed by Schwarz in 1980 in a pulsed radiolysis of a gas cell containing ammonia in a helium carrier.[16]

Schwarz's measurements made use of the known equilibrium constants for the clustering reactions to deconvolute the absorption signal obtained at various pressures into those of individual ammoniated ammonium ions. These pioneering measurements, discussed later in the context of the results of the present study, suffered from limited spectral resolution (40-$cm^{-1}$ full width at half-maximum (fwhm)), relatively high vibrational and rotational temperatures (>300 K), and some ambiguity regarding the distribution of cluster sizes present in the sample. Nonetheless, it was possible for Schwarz to observe the vibrational bands $\nu_3$ and $2\nu_4$ of the ammonium ion core for the $n$ = 4 cluster and to show that the $n$ = 3 spectrum was consistent with $C_{3v}$ symmetry. Schwarz was able to prove by isotope substitution that the structure of the $n$ = 4 ion cluster is tetrahedral. No transitions were observed that could unambiguously be assigned to the solvent molecules surrounding the ammonium ion.

Recently, we have studied the infrared vibrational predissociation spectroscopy of the tetraammoniated ammonium ion $NH_4^+(NH_3)_4$ using an arrangement of tandem mass spectrometers, a radio-frequency (rf) ion trap, and a tunable infrared laser.[17] In addition to simply vibrational transitions, we have observed spectral features that are due to nearly free internal rotation of the ammonia subgroups in $NH_4^+(NH_3)_4$, the first observation of such a phenomenon in an ionic cluster. This work also served to verify Schwarz's spectrum determined by deconvolution of the time-dependent infrared absorbance based on equilibrium and rate constants and his assignment of the $\nu_3$ and $2\nu_4$ bands in the spectrum. The comparison with our spectra further indicates that the spectra we derive from vibrational predissociation are similar to those obtained by direct absorption for this system. In the present work we give a full account of our systematic investigation of a series of infrared vibrational predissociation (IRVPD) spectra of the ammoniated ammonium ions and present the absorption spectra for $NH_4^+(NH_3)_n$ ($n$ = 1–10) over the frequency range 2600–3500 $cm^{-1}$.

It will be shown that correlation of spectral features with cluster size can provide information about solvation shell structure, the geometry of the clusters, and the onset of a condensed-phase

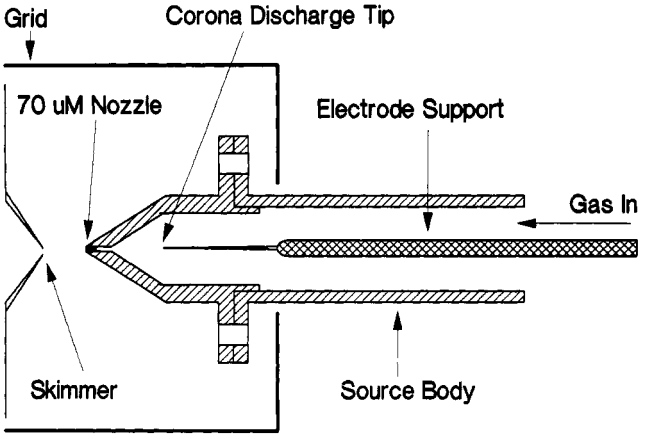


**Figure 2.** Schematic diagram of the ion source, which consists of a corona discharge and supersonic expansion.

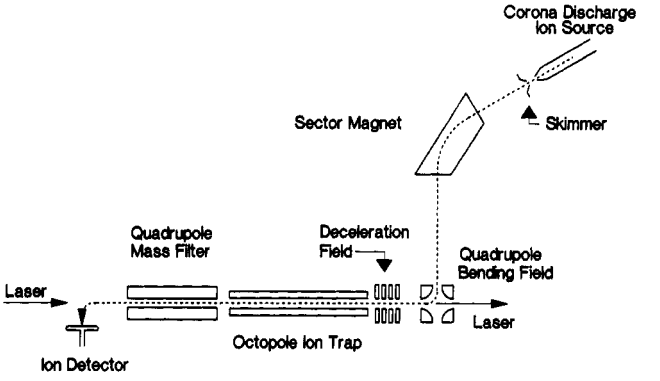


**Figure 3.** Schematic diagram of the experimental apparatus.

environment around the ion core. With sufficient laser resolution, rotational information about the cluster should also be obtainable with this new experimental technique.

## Experimental Details

The experimental apparatus used in this work has been described previously.[18-21] Briefly, the ammoniated ammonium cluster ions were produced from a high-pressure corona discharge source and subsequent supersonic expansion. Schematic diagrams of the source and the experimental apparatus are shown in Figures 2 and 3. The corona discharge was maintained in 100–200 Torr of gas (Matheson ultrahigh purity (UHP) neon typically seeded with 10% UHP $H_2$ and about 1% $NH_3$) flowing past a 1.2-kV potential from the discharge tip of the needle to the source body maintained at approximately 350 V above ground. The discharge current under these conditions ranged from 40 to 200 $\mu$A. The source could be cooled from outside the machine by contact with a liquefied gas reservoir and was usually maintained at approximately −30 °C. After passing through the discharge region, the ionized gas undergoes collisionally induced vibrational relaxation in the 1.0-mm-long by 3.0-mm-diameter drift region before expanding through the 70-$\mu$m expansion nozzle. It is estimated that an ion undergoes some $10^5$ collisions in this region before leaving the source, resulting in the ion relaxing to a vibrational temperature near that of the source body by the time it reaches the nozzle.

Most of the clustering of the neutral gas around the ionic species and rotational cooling takes place during the supersonic expansion between the nozzle and the skimmer. Typical pressures in the

(14) Crofton, M. W.; Oka, T. *J. Chem. Phys.* **1983**, *79*, 3157; **1987**, *86*, 5983.
(15) Schafer, E.; Saykally, R. J. *J. Chem. Phys.* **1984**, *80* (9), 3969.
(16) Schwarz, H. A. *J. Chem. Phys.* **1980**, *72*, 284.
(17) Price, J. M.; Crofton, M. W.; Lee, Y. T. *J. Chem. Phys.* **1989**, *91*, 2749.
(18) Bustamente, S. W. Ph.D. Thesis, University of California at Berkeley, 1983.
(19) Bustamente, S. W.; Okumura, M.; Gerlich, D.; Kwok, H. S.; Carlson, L. R.; Lee, Y. T. *J. Chem. Phys.* **1987**, *86*, 508.
(20) Okumura, M. Ph.D. Thesis, University of California at Berkeley, 1986.
(21) Yeh, L. I.-C. Ph.D. Thesis, University of California at Berkeley, 1988.

source chamber are $4 \times 10^{-5}$ to $2 \times 10^{-4}$ Torr while running the experiment. To prevent internal excitation and dissociation of the ionic clusters through collisions with the background gas in the expansion, the potential of the skimmer was maintained within 5 V of that of the source body. A shielding grid surrounding the expansion region maintained at 350 V prevented stray fields from affecting the ion trajectories in this region.

After the skimmer, the ion beam enters a second differential pumping region containing collimating and focusing optics. The pressure in this second region is typically an order of magnitude lower than that of the source region. The beam is then directed into a third differentially pumped region maintained at $10^{-8}$ Torr and through the entrance slits of a 60° sector magnet mass analyzer (resolution = $M/\Delta M \approx 200$). To aid in transmission of the ion beam and to enhance mass resolution, a set of quadrupole lens pairs is placed before and after the magnet.[22,23]

The mass-selected beam passes into the final differentially pumped region maintained at $10^{-9}$ Torr. Here, the beam is bent 90° in a dc quadrupole field, decelerated to less than 0.5 eV, and focused into a rf octopole ion trap through an entrance aperture lens. Ions are typically allowed into the trap for 1 ms before the potential of the entrance lens is raised, and the ions are confined inside the octopole.

The confined, mass-selected clusters are then vibrationally excited by a pulsed, tunable infrared laser. (Quanta Ray, IR WEX 8-ns pulse, 0.3–1.2-$cm^{-1}$ resolution, 0.7-$cm^{-1}$ absolute frequency accuracy, 0.2–1.0 mJ/pulse in the 2600–4000-$cm^{-1}$ region). The density of ionic clusters in the ion trap is not high enough to allow the measurement of photon absorptions directly. In order to detect the absorption of an IR photon by an ionic cluster, IR multiphoton dissociation processes were used to exclusively dissociate the vibrationally excited ionic clusters. Depending on the density of states and the dissociation energy of the species under study, one of two excitation schemes described below was employed.

Because of the large binding energies of the $n = 1$ and 2 ammoniated ammonium ions, absorption of sufficient energy from the tunable infrared (IR) laser to cause predissociation is not a facile process. In these cases, a line tunable $CO_2$ laser is used (MPB Technologies Inc., 8 W CW on R(24) of the $00^01$–$02^00$ transition) to drive the clusters excited by the tunable IR laser over the dissociation limit through the absorption of multiple $CO_2$ laser photons. This process hinges on the initial absorption of the tunable IR photon, as the density of states 1000 $cm^{-1}$ above the $v = 0$ level is so low that multiphoton dissociation of the ionic clusters by the CW $CO_2$ laser alone is very unlikely even with tens of milliseconds of irradiation time. In the studies of the $n = 1$ cluster, no vibrational predissociation signal was observed if the pulsed laser was not present. Further discussion of this technique may be found elsewhere.[21]

For the larger clusters, $n = 3$–10, the energy required to predissociate one solvent molecule is exceeded by absorbing two photons in the usual tuning range of 2.5–3.8 μm. At an energy in the 2600–4000-$cm^{-1}$ region, all of the ionic clusters ($n = 1$–10) are literally in the "quasi-continuum" region[24] after the absorption of one photon, and an additional IR photon from the tunable laser may be absorbed to induce vibrational predissociation. For $n = 1$ and 2, however, fragments were not detectable with the tunable laser only, presumably because the fluence was not sufficient for the absorption of more than two photons. For these ions, use of the $CO_2$ laser with an irradiation time of at least 10 ms at >10 $W/cm^2$ was required to achieve a measurable degree of dissociation of vibrationally excited clusters. In those instances where spectra of a given ion were obtained by both one- and two-color schemes, they were found to be the same within experimental error, indicating that spectral features in the multiphoton dissociation spectra normally reflect the cross section for absorption of the first photon rather well.[21]

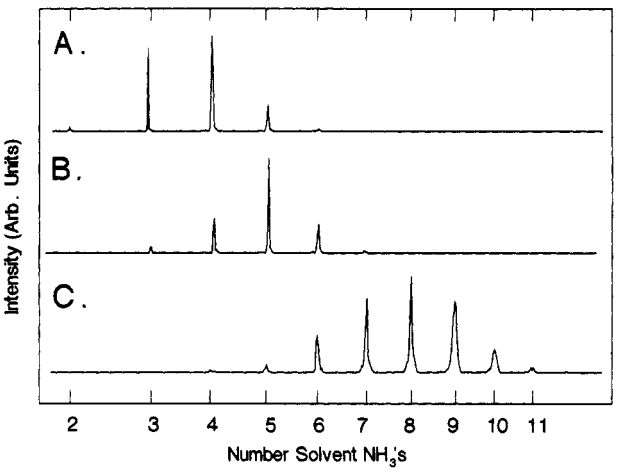


**Figure 4.** Mass spectra showing the $NH_4^+(NH_3)_n$ cluster distribution as a function of ion source conditions. For (a), the $NH_3/H_2/Ne$ mixture flowed through a liquid nitrogen trap to reduce the $NH_3$ concentration. The source backing pressure was raised to obtain (b), and the trap was bypassed to obtain (c). The $NH_3/H_2/Ne$ mixture was ≈1:10:100.

If the clusters absorb sufficient energy through one of the schemes described above, the loss of one or more solvent molecules from the parent cluster may occur. The potential on the exit aperture is lowered 1 ms after the laser pulse, extracting cluster ions of all masses from the trap. These ions are filtered by a second mass analyzer, a quadrupole mass spectrometer tuned to pass only the daughter ions smaller than the parent cluster by one solvent molecule.

Daughter ions are counted by means of a Daly ion detector[25] for each laser shot. Background daughter ion counts resulting from the decay of metastable parent ions in the rf ion trap are monitored in a separate data cycle with the laser off at each wavelength and subtracted from the laser on signal. Typical background count rates usually amount to no more than 1% of the signal at the stronger absorption maxima. The spontaneous decay of metastable parent ions to daughter ions in the trap was as high as 5% for the largest ions and as low as $10^{-2}$% for $NH_4^+(NH_3)$.

Laser power is monitored at each data point, and spectra are normalized for the tunable infrared power by using a simple linear power dependence. For a typical experiment, signals were averaged for about 400 laser shots at each wavelength in the 2600–3200-$cm^{-1}$ region and longer and about 1000 laser shots at each wavelength in the 3200–4000-$cm^{-1}$ region where signals were typically much weaker. This extra averaging is reflected in the better signal-to-noise ratios in the higher frequency region for some of the traces shown in Figure 9. Relative intensities between the two frequency regions should be correct.

## Results and Discussion

*A. Mass Spectra.* The distribution of ionic clusters produced by the corona discharge source could be shifted by altering the temperature of the source body, the backing pressure of the supersonic expansion, or the percentage of $NH_3$ in the $H_2$ carrier gas. Little dependence was observed between the peak of the cluster ion distribution and the magnitude of the current used in the discharge for a given value of the above parameters, indicating that the ions were at a reasonable equilibrium with the temperature of the source body before expansion through the nozzle.

The distribution of cluster sizes produced by the source could be easily monitored by sweeping the field of the 60° sector magnet and counting the ions that arrive at the Daly detector with the second mass filter set to transmit all ions. Two such mass spectra

(22) Enge, H. A. *Rev. Sci. Instrum.* **1959**, *30*, 248. Giese, C. F. *Ibid.* **1959**, *30*, 260. Lu, C.-S.; Carr, H. E. *Ibid.* **1962**, *33*, 823.

(23) Taya, S.; Kanomatata, I.; Hirose, H.; Noda, T.; Matsuda, H. *Int. J. Mass Spectrom. Ion Phys.* **1978**, *26*, 237.

(24) Demtröder, W. *Laser Spectroscopy: Basic Concepts and Instrumentation*; Springer-Verlag Press: New York, 1982. Letokhov, V. S. *Nonlinear Laser Chemistry: Multiple-Photon Excitation*; Springer-Verlag Press: New York, 1983.

(25) Daly, R. N. *Rev. Sci. Instrum.* **1960**, *31*, 264.

are shown in Figure 4. Spectrum a was taken with a low concentration of ammonia in the $H_2$ carrier gas (<1%), a backing pressure of 200 Torr behind the nozzle, and the source body cooled to −30 °C through contact with liquid freon 12. For these conditions the distribution shows a peak at the $n$ = 4 cluster. When the source is cooled with liquid freon 22 (−40 °C) instead of freon 12, and a higher pressure is used behind the nozzle, larger cluster ions could be favored as shown in Figure 4c. Figure 4b shows an intermediate condition. In this manner it was possible to produce in relatively high numbers the range of ionic cluster sizes desired for this study.

*B. Notation for Spectral Assignments.* Of the various vibrational motions that take place within the ammoniated ammonium cluster ions, the only fundamental vibrational transitions accessible to the present laser system involve the high-frequency N–H stretching motions. The numerous low-frequency bending motions available to the cluster are in the case of this work observed only as overtone absorptions or in combination with a high-frequency stretch. The higher frequency stretches we have assigned involve two types of N–H oscillators: those associated with the $NH_4^+$ core and those of the $NH_3$ solvent molecules.

For each of these, the frequency of a given transition for a particular subunit (either $NH_4^+$ or $NH_3$) will be shifted from that of the free molecule (or ion) by an amount determined by the local environment around the absorbing species. The normal modes of the $NH_4^+$ ion will be split into lower and higher frequency components due to the bound N–H's and higher frequency components associated primarily with bound and free N–H oscillators, respectively. Similarly, the $NH_3$ solvent molecules in the first solvation shell ($n \leq 4$) will be strongly influenced by $NH_3$ molecules in the second solvation shell and beyond ($n > 4$).

Because of the lengthy descriptions required to indicate the assignment of many of the vibrational bands, we introduce a shorthand notation: ${}^{y}X^{\circ}$ N–$H_p^z$ to designate the subgroup involved in a particular transition and to describe the type of vibrational motion the subgroup undergoes. Under this notation, $X$ takes on the values 0, 1, 2, ... and indicates whether the subgroup is in the core, first solvation shell, second solvation shell, etc., $y$ is the number of equivalent N–H oscillators of a particular bond type *in the local subunit*, $z$ is either bd (bound) or fr (free) to indicate whether the H of the N–H bond is involved in hydrogen bonding, and $p$ is sstr, astr, or bend depending upon whether the vibration can be considered as a symmetric or an antisymmetric stretch or a bending mode *in the local subunit*. If the symmetry of the stretch is not determined, but we still consider the transition a stretching type vibration, we omit the s or the a in the notation. If a bond is directly affected by two attached subunits, where one of the subunits attaches to the other, $z$ takes the form bd,bd. Our notational system can be used for spectra of other ion clusters as well, by adapting the N–H designation to indicate the appropriate bond type. Such a system treats the vibrational modes of each subunit separately from the rest of the complex. This "local subunit" approximation seems to work well for labeling spectra of weakly bound clusters, at least for the present spectral resolution. We will also use more conventional labels and full descriptions in many cases, reserving the most extensive use of the new notation for our table of assignments.

*C. Infrared Vibrational Spectra.* In analyzing the infrared spectra of the ammoniated ammonium ion series, it is helpful to examine the general trends observed in the spectra before delving into a detailed investigation of individual cases. As implied by the notational scheme presented in the previous section, our approach has been to treat the various subunits in the cluster as essentially isolated molecules ($NH_3$ or $NH_4^+$) perturbed by their particular environment. This approach is helpful from the standpoint of visualizing the types of vibrations involved in a given transition and frees us from thinking of these large systems in terms of a normal-mode type of picture when the weak coupling between the subunits makes such an analysis difficult for all but the smallest clusters (e.g, $n$ = 1 and 2).

The spectra of the ammoniated ammonium ion series show a number of common features. Both absorptions due to the ammonium core stretches and those due to the ammonia solvent molecules can be assigned in every case. Features of the $NH_4^+$ core assigned to vibrations involved in hydrogen bonds with the solvent $NH_3$'s are strongly red-shifted from the gas-phase values obtained from velocity modulation spectroscopy[13-15] due to the strong interactions of the N–H bonds of the ion with the solvent molecules. Vibrational transitions involving the $NH_3$ molecules in the first solvation shell (1°) of the complex are significantly less perturbed from their gas-phase values, however, because the N–H bonds of the ammonias are not themselves involved in the hydrogen bond. This situation is changed for an N–H bond of the 1° ammonia which is involved in a hydrogen bond with a second solvation shell (2°) ammonia. A larger red shift will take place for that N–H bond of the 1° ammonia, although not as large as that for the ion.

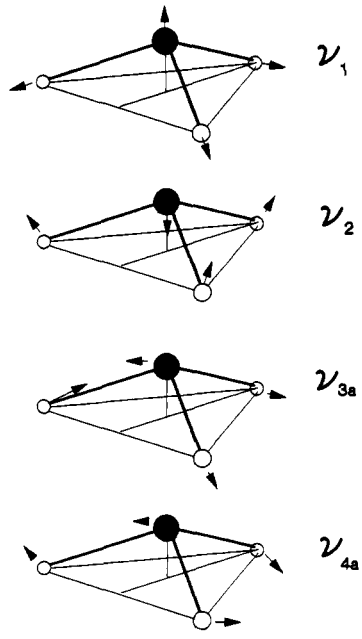


**Figure 5.** Normal modes of $NH_3$. Only one linear combination has been shown for the doubly degenerate modes $\nu_3$ and $\nu_4$. Again, arrows in the figure indicate the direction of motion but are not to scale for the amplitude of the motion. (See ref 38.)

The spectral features due to the ion core in particular and to a lesser extent the solvent molecules show some systematic trends with increasing cluster size. The ion core frequencies associated with extensive hydrogen bonding show a gradual blue shift. The amount of this shift is not constant with increasing solvation, however, and in the extreme case of the largest clusters ($n$ = 9–10), the spectra change very little between the addition of one solvent molecule and the next, indicating that the core of the system is perhaps converging toward a liquidlike state.

The most striking feature of the spectra between 2600 and 3500 $cm^{-1}$ for $n$ = 1–6 is a band originating at roughly 3400 $cm^{-1}$ composed of a number of resolved subbands having a separation between adjacent components of about 12 $cm^{-1}$. This spacing is about twice the rotational constant for $NH_3$ about its $C_3$ symmetry axis and arises from the nearly free internal rotation of the 1° solvent molecules within the cluster. Observed previously in the $NH_4^+(NH_3)_4$ spectrum,[17] and assigned to a perpendicular band corresponding to the $\nu_3$ mode of free $NH_3$ (see Figure 5), these transitions indicate that some of the solvent molecules in the first solvation shell are relatively unhindered even when the second solvation shell has begun to fill.

The assignments of the internal rotation subbands were given for $NH_4^+(NH_3)_4$ and are analogous for the corresponding bands of the other cluster ions. We use the notation for a strongly prolate symmetric top rotor in the table of assignments (see Table III) and in the text to describe the subbands. When the transitions ${}^{R}Q_3$ and ${}^{P}Q_3$ are observable, their intensities are consistent with the expected spin weight for transitions in $NH_3$ originating from $K$ = 3 levels. The only vibrational transitions for which the internal

**TABLE III: Vibrational Frequencies (in cm$^{-1}$) for the Ammoniated Ammonium Ions[a]**

| this work | previous work | assignment |
|---|---|---|
| | | $NH_4^+(NH_3)$ |
| 3376.6 | | $^PQ_2$ |
| 3377.4 | | |
| 3387.0 | | $^PQ_1$ |
| 3387.8 | | |
| 3397.4 | 3420 (sh) | $^RQ_0$ } $NH_3$ $\nu_3$ asym str |
| 3398.2 | | |
| 3409.2 | | $^RQ_1$ |
| 3419.5 | | $^RQ_2$ |
| 3392.0 | | $^PR_1(J)$? (see text) |
| 3402.1 | | $^RR_0(J)$? (see text) |
| 3412.4 | | $^RR_1(J)$? (see text) |
| | | $NH_4^+(NH_3)_2$ |
| 3392.0 | | $^PQ_2$ of $NH_3$ $\nu_3$ overlapped with $NH_4^+$ free N–H asym str |
| 3395.4 | 3360 | $NH_4^+$ free N–H asym str |
| 3401.9 | | $^PQ_1$ |
| 3413.7 | | $^RQ_0$ } $NH_3$ $\nu_3$ asym str |
| 3425.8 | | $^RQ_1$ |
| 3426.8 | | |
| | | $NH_4^+(NH_3)_3$ |
| 2615 | | $NH_4^+$ $\nu_1'$ ($^30°$ N–$H^{bd}_{astr}$)? |
| 2660 | | $NH_4^+$ $\nu_1'$ ($^30°$ N–$H^{bd}_{astr}$) or $\nu_3''$ ($^30°$ N–$H^{bd}_{astr}$) |
| 2692 | | $NH_4^+$ $\nu_1'$ ($^30°$ N–$H^{bd}_{astr}$) or $\nu_3''$ ($^3O°$ N–$H^{bd}_{astr}$) |
| 3374.1 | 3365 | $NH_4^+$ free N–H str $\nu_3'$ ($^10°$ N–$H^{fr}_{astr}$) |
| 3390.8 | | $^PQ_2$ |
| 3393.1 | | |
| 3404.2 | | $^PQ_1$ |
| 3404.9 | | |
| 3416.8 | | $^RQ_0$ } $NH_3$ $\nu_3$ asym str |
| 3429.0 | | $^RQ_1$ |
| 3429.9 | | |
| 3439.6 | | $^RQ_2$ |
| 3452.3 | | $^RQ_3$ |
| | | $NH_4^+(NH_3)_4$ |
| 2865 | 2867 | $NH_4^+$ asym str $\nu_3$ ($^40°$ N–$H^{bd}_{astr}$) |
| 3095 | 3087 | $NH_4^+$ bend $2\nu_4$ ($^40°$ N–$H^{bd}_{bend}$) |
| 3383.0 | | $^PQ_3$ |
| 3384.3 | | |
| 3393.5 | | $^PQ_2$ |
| 3394.2 | | |
| 3407.8 | | $^PQ_1$ |
| 3408.4 | | |
| 3420.5 | | $^RQ_0$ } $NH_3$ $\nu_3$ asym str |
| 3432.8 | | $^RQ_1$ |
| 3433.3 | | |
| 3443.3 | | $^RQ_2$ |
| 3444.1 | | |
| 3454.9 | | $^RQ_3$ |
| 3456.5 | | |
| | | $NH_4^+(NH_3)_5$ |
| 3650 | | $NH_4^+$ $\nu_3''$ str ($^10°$ N–$H^{bd,bd}_{str}$) |
| 2880 | | $NH_4^+$ $\nu_3'$ sym str ($^30°$ N–$H^{bd}_{astr}$) |
| 2910 | | $NH_4^+$ $\nu_1'$ asym str ($^30°$ N–$H^{bd}_{astr}$) |
| 3010 (two peaks) | | see text for tentative assignt |
| 3110 (two peaks) | | $NH_4^+$ bend overtone (see text) |
| 3228 | | overlap of $NH_3$ $2\nu_4$ and $^11°$ N–$H^{bd}_{str}$ |
| 3364.4 | | $NH_3$ free N–H asym str ($^21°$ N–$H^{fr}_{astr}$) |
| 3382.7 | | $^PQ_3$ |
| 3383.8 | | |
| 3394.1 | | $^PQ_2$ |
| 3395.2 | | |
| 3407.2 | | $^PQ_1$ } $1°$ $NH_3$ $\nu_3$ asym str |
| 3408.2 | | |
| 3419.8 | | $^RQ_0$ |
| 3433.0 | | $^RQ_1$ |
| 3443.5 | | $^RQ_2$ |
| 3455.6 | | $^RQ_3$ |
| 3456.3 | | |
| | | $NH_4^+(NH_3)_6$ |
| 2720 | | $^20°$ N–$H^{bd,bd}_{astr}$ |
| 2910 | | $^20°$ N–$H^{bd}_{astr}$ |
| 2950 | | $^20°$ N–$H^{bd}_{astr}$ |
| 3020 | | $NH_4^+$ bend overtone |
| 3228 | | $1°$ $NH_3$ H-bonded str ($^11°$ N–$H^{bd}_{str}$) |
| 3368.4 | | $1°$ $NH_3$ free N–H str ($^21°$ N–$H^{fr}_{astr}$) |
| 3398.2 | | $^PQ_2$ |
| 3410.8 | | $^PQ_1$ |
| 3423.7 | | $^RQ_0$ } $1°NH_3\nu_3$ asym str |
| 3435.7 | | $^RQ_1$ |
| 3448 | | $^RQ_2$ |
| | | $NH_4^+(NH_3)_7$ |
| 2770 | | $^30°$ N–$H^{bd,bd}_{astr}$ |
| 2870 | | combination of above with hydrogen bond str |
| 2955 | | $^10°$ N–$H^{bd}_{str}$ |
| 3050 | | $NH_4^+$ bending overtone |
| 3220 | | $^11°$ N–$H^{bd}_{str}$ |
| 3375 | | $^21°$ N–$H^{fr}_{astr}$ |
| 3415 | | overlap of $^31°$ N–$H^{fr}_{astr}$ and $^32°$ N–$H^{fr}_{astr}$ (?), unable to assign subbands for $^31°$ N–$H^{fr}_{astr}$ |
| | | $NH_4^+(NH_3)_8$ |
| 2820 | | $^40°$ N–$H^{bd,bd}_{astr}$ ($NH_4^+$ $\nu_3$) |
| 2910 | | combination of above with hydrogen bond str? |
| 3050 | | $^40°$ N–$H^{bd,bd}_{bend}$ overtone ($NH_4^+$ $2\nu_4$) |
| 3220 | | $^11°$ N–$H^{bd}_{str}$ for each of four "identical" subunits, possible overlap from $2°$ $NH_3$ $2\nu_4$ |
| 3300 | | $^21°$ N–$H^{fr}_{astr}$? |
| 3320 | | $^21°$ $NH_3$ $\nu_1$ ($^32°$ N–$H^{f}_{str}$)? |
| 3380 | | $^21°$ N–$H^{fr}_{astr}$ |
| 3415 | | $2°$ $NH_3$ $\nu_3$ ($^32°$ N–$H^{fr}_{astr}$) |
| | | $NH_4^+(NH_3)_9$ |
| 2829 | | $NH_4^+$ $\nu_3$ asym str |
| | | $NH_4^+(NH_3)_{10}$ |
| 2841 | | $NH_4^+$ $\nu_3$ asym str |

[a] Experimental frequencies from this work were found by using the IRMPD technique.

rotor state of $NH_3$ will change are those involving modes of $NH_3$ with the selection rule $\Delta K = \pm 1$; here $K$ is the quantum number for angular momentum about the $NH_3$ $C_3$ axis. (Our use of $K$ and the notation $^{R,P}Q_K$, as we have stated previously,[17] is not strictly correct. We use it for convenience, as the notation follows easily from the picture of $NH_3$ attached to a "wall", perpendicular to its $C_3$ axis. In the standard treatment presented here for the internal rotation observed in $NH_4^+(NH_3)$, both $K$ and $K_i$, the internal rotation quantum number, must be used, and the symmetry and interaction of the rest of the molecule must be included. There is no well-developed theory for the treatment of the larger clusters.) No vibration of the ammonium core species carries this selection rule for angular momentum about one of the $NH_3$ $C_3$ axes; only a perpendicular vibration of the $NH_3$ subunit satisfies the condition. This includes the $\nu_3$ type fundamental but not $\nu_1$ (see Figure 5). It also includes the $\nu_4$ type fundamental of $NH_3$ (the frequency is too low for us to observe) and perpendicular components of overtone and combination bands. The overtone $2\nu_4$ could therefore have shown the characteristic 12-cm$^{-1}$ spacing, but did not. The most intense component of $2\nu_4$ is probably a parallel band. A detailed treatment of the internal rotation of the simpler $n = 1$ cluster ion is given along more standard lines.

For $n \geq 4$, fundamental bands in the 3150–3500-cm$^{-1}$ region derive entirely from perturbed ammonia subunits. In the region

2600–3150 $cm^{-1}$, only vibrations associated with the $NH_4^+$ core appear. $NH_4^+$ is strongly hydrogen-bonded via its hydrogen atoms, resulting in a large red shift of the N–H stretching frequencies. The N–H vibrational frequencies in $NH_3$ shift relatively little when binding to the $NH_4^+$ core since the nitrogen atom of ammonia binds, rather than hydrogen. The hydrogen bonding between first shell (1°, primary) and second shell (2°, secondary) $NH_3$ is relatively weak; therefore, the frequency shift of the bonded N–H stretch of 1° $NH_3$ is also relatively small. The separation of $NH_3$ and $NH_4^+$ vibrational bands for $n \geq 4$ in the 2600–3500-$cm^{-1}$ region is therefore easily understandable. This separation of core and solvent bands, taken together with the way in which several bond types form well-behaved series as a function of $n$, simplified the assignment process considerably.

The infrared absorption spectra for $NH_4^+(NH_3)_n$ ($n$ = 1–10) are discussed in detail below. Observed transition frequencies and assignments of the vibrational and rovibrational transitions observed in these spectra appear in Table III. Where available, observations from previous work are included in the table. Representative spectra for the $n$ = 1–8 ionic cluster series appear in Figures 6 and 9 and are discussed in detail for each cluster in the following text.

*1. $NH_4^+(NH_3)$.* The smallest ionic cluster studied in this work is the ammonium ion solvated by a single ammonia. Bound with a $\Delta H°$ of formation of −27 kcal/mol, it is the most strongly bound of the ammoniated ammonium cluster ion series. Due to its small number of low-frequency vibrational modes, the density of states[26] is expected to be rather low at 3500 $cm^{-1}$. Like the analogous hydrated hydronium ion, it is important to know the equilibrium position of the proton between the two heavier nitrogen atoms. The two possible structures for this simplest cluster appear in Figure 7. In the $C_{3v}$ structure, the proton is localized around one of the ammonias, suggesting that the appropriate formulaic description of this system would be $NH_4^+(NH_3)$, whereas in the $D_{3h}$ structure ($D_{3d}$ is probably a more stable conformation by perhaps 10 $cm^{-1}$) it is equally shared, suggesting that $(H_3N)H^+(NH_3)$ is the appropriate representation.

Ab initio calculations for the structure of the analogous $H_3O^+(H_2O)$ cluster ion suggested a double or single minimum for the proton position depending on the level of the calculation. The most sophisticated calculation to date is the as yet unpublished work of the Schaefer group in which the energies of the $C_2$ and $C_s$ structures were found to have energies differing by no more than a few kcal/mol.[27] At the highest level of theory (full CISD—configuration interaction including single and double excitations) the single minimum (symmetric $H_5O_2^+$ where the proton is at the midpoint of the oxygen atoms) was favored. At low levels of theory, the symmetric structure is usually favored also, but this order does not always hold.[27–31] Spectroscopic investigations performed in this laboratory concluded that in this case the proton was centrally located,[32,33] i.e., associated with a single-minimum potential. Much evidence for the existence of such a structure in the solid and liquid phases has been presented previously in the literature.[34] One of the most plausible proposals for the mechanism of proton transfer in aqueous acid solutions requires the existence of the symmetric structure, at least as a transition state. Knowledge of the function that describes the potential energy for the proton as a function of its position and the O–O separation is critical to understand and evaluate such a mechanism.

Theoretical calculations on $NH_4^+(NH_3)$ are significantly more primitive than those used for $H_5O_2^+$ but predict $N_2H_7^+$ to have an asymmetric $C_{3v}$ structure.[35,36] The calculated energy difference, once again, is only a few kcal/mol. Given the margin for error in such a calculation and the fact that $N_2H_7^+$ and $H_5O_2^+$ are isoelectronic and obviously very similar molecules, such a conclusion cannot be accepted without verification. Both species have been theoretically studied extensively by Scheiner to determine the potential energy with respect to the proton position and the N–N or O–O separation. His results show that the potential and its form depend much more strongly on the N–N or O–O separation than the proton position, with respect to which the potential energy is extremely flat.

Assuming a symmetric structure ($D_{3h}$, see Figure 7b) for this ion, the most intense absorption involving a high-frequency N–H stretching motion would probably be the antisymmetric stretch of the $NH_3$ subunits. This motion, analogous to the $\nu_9$ and $\nu_{13}$ modes in 2-butyne (dimethylacetylene), would give rise to a degenerate perpendicular transition of $E_{1d}$ and $E_{2d}$ symmetry. From the standpoint of one of the ammonias, this motion is analogous to the doubly degenerate antisymmetric stretch, $\nu_3$, of free ammonia, which occurs at 3444 $cm^{-1}$ in the gas phase[37] (see Figure 5). The asymmetric structure for the dimer, in contrast ($C_{3v}$, see Figure 7a), would have at least two types of antisymmetric stretching vibrations, one associated with the H-bonded $NH_4^+$ ion and one associated with the $NH_3$ molecule.

Schwarz detected a weak absorption as a shoulder at 3420 $cm^{-1}$ that he assigned to this cluster. Any band arising from a stretching motion involving the hydrogen-bonded proton evidently occurs below 2000 $cm^{-1}$ and was not observed. The transition we observed for this system appears in Figure 6a and is centered at 3398.4 $cm^{-1}$, in reasonable agreement with the weak feature in Schwarz's spectrum at 3420 $cm^{-1}$. Schwarz assigned this to be $\nu_1$ of the $NH_3$ subunit.

At the higher resolution available to this study, we found this band to be composed of a series of subbands spaced by 10.6 ± 0.3 $cm^{-1}$. For a prolate symmetric top molecule with the rotational constants $A >> B = C$, a strong Q-branch progression of this kind superimposed on vibrational transitions is commonly observed.[38] Spectra for molecules of this type, such as $CH_3Br$, have a characteristic separation between the Q-branch maxima of approximately 2 $(A - B)$.[39]

For the structure observed in the $N_2H_7^+$ spectrum to be due to a simple rotation of the dimer, however, the spacing of the subbands should be ≈5.6 $cm^{-1}$, based on the ab initio equilibrium geometry.[12] The fact that the actual spacing is roughly twice as large and that similar structure was observed previously in the much larger $n$ = 4 cluster ($A = B = C \approx 0.1$ $cm^{-1}$) suggests that these bands are due to an internal rotation of the $NH_3$ subgroups about their local $C_3$ axes, similar to that observed in $NH_4^+(NH_3)_4$.[17]

*Internal Rotation in $NH_4^+(NH_3)$.* Internal rotation of molecules containing $C_3$ subgroups has been given extensive theoretical treatment.[40] Theories developed by Longuet-Higgins and Bunker[41] and Papousek[42,43] have been used to explain the structure in the antisymmetric stretching band, $\nu_9$, $\nu_{13}$, in 2-butyne attributed to internal rotation of the methyl subgroups. In these theories,

(26) Robinson, P. J.; Holbrook, K. A. *Unimolecular Reactions*; Wiley-Interscience: New York, 1972.
(27) Remington, R.; Schaefer III, H. F. Unpublished results.
(28) Newton, M. D.; Ehrenson, S. *J. Am. Chem. Soc.* **1971**, *93*, 4971.
(29) Newton, M. D. *J. Chem. Phys.* **1977**, *67*, 5535.
(30) Potier, A.; Leclercq, J. M.; Allavena, M. *J. Phys. Chem.* **1984**, *88*, 125.
(31) Yukhnevich, G. V.; Kokganova, E. G.; Pavlyuchko, A. I.; Volkov, V. V. *J. Mol. Struct.* **1985**, *122*, 1.
(32) Okumura, M.; Yeh, L. I.-C.; Meyers, J. D.; Lee, Y. T. *J. Chem. Phys.* **1986**, *85*, 2328.
(33) Yeh, L. I.-C.; Okumura, M.; Myers, J. D.; Price, J. M.; Lee, Y. T. *J. Chem. Phys.* **1989**, *91* (12), 7319.
(34) Ratcliffe, C. I.; Irish, D. E. *Water Science Reviews*; Franks, F., Ed.; Cambridge University Press: Cambridge, 1986; Vol. 2; 1988, Vol. 3.
(35) Scheiner, S.; Harding, L. B. *J. Am. Chem. Soc.* **1981**, *103*, 2169.
(36) Hirao, K.; Fujikawa, T.; Konishi, H.; Yamabe, S. *Chem. Phys. Lett.* **1984**, *104*, 184.
(37) Benedict, W. S.; Phyler, E. K.; Tidwell, E. D. *J. Chem. Phys.* **1960**, *32*, 32.
(38) Herzberg, G. *Infrared and Raman Spectroscopy*; Van Nostrand: Princeton, 1945.
(39) Bennett, W. F.; Meyer, C. F. *Phys. Rev.* **1928**, *32*, 888.
(40) Owen, N. L. Studies of Internal Rotation by Microwave Spectroscopy. In *Internal Rotation In Molecules*; Orville-Thomas, W. J., Ed.; Wiley-Interscience: New York, 1974.
(41) Bunker, P. R.; Longuet-Higgins, H. C. *Proc. R. Soc. London, Ser. A* **1964**, *280*, 340.
(42) Papousek, D. *J. Mol. Spectrosc.* **1968**, *28*, 161.
(43) Olson, W. B.; Papousek, D. *J. Mol. Spectrosc.* **1971**, *37*, 527.

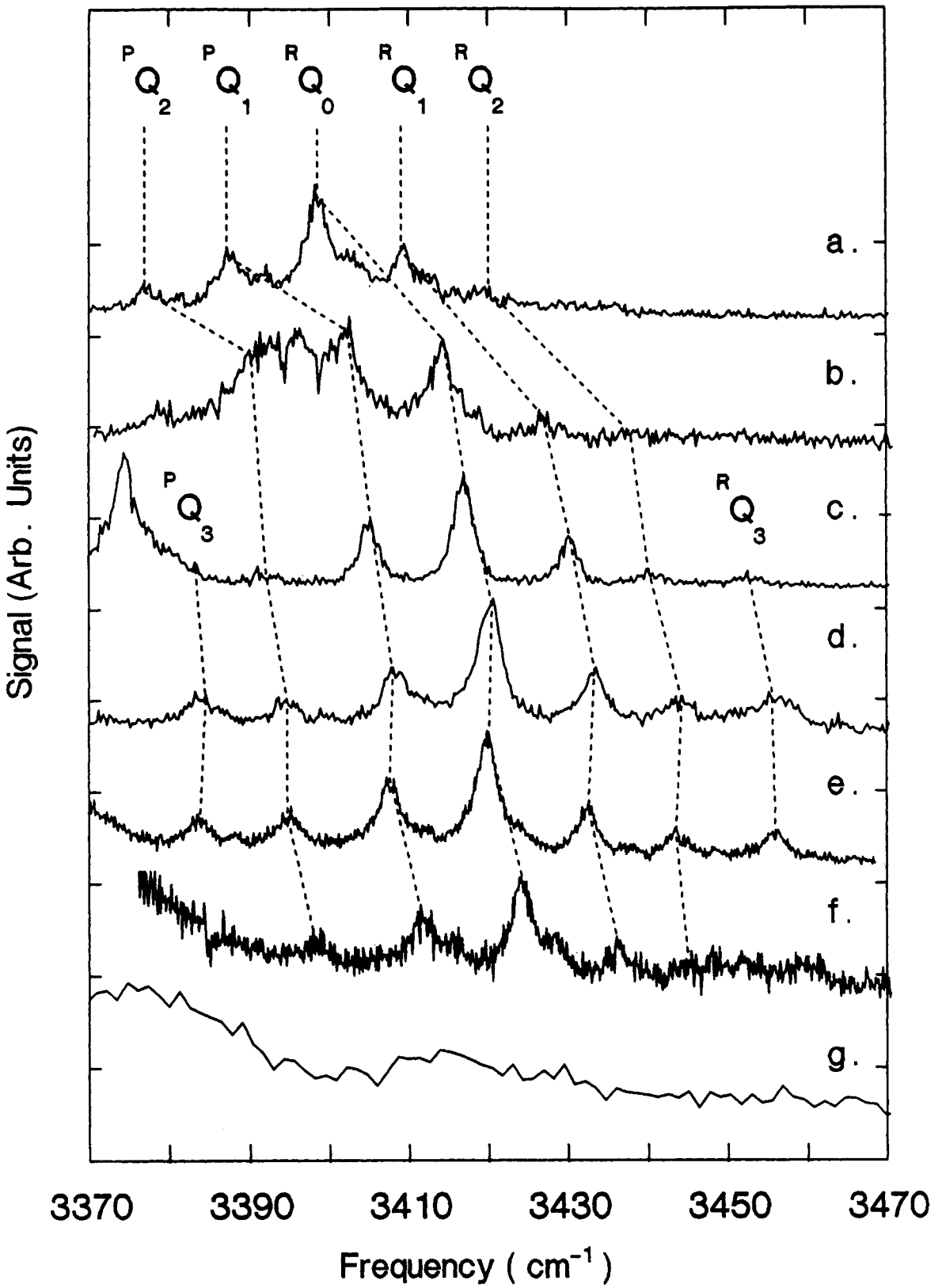


**Figure 6.** Vibrational predissociation spectra of $NH_4^+(NH_3)_n$ ($n$ = 1–6 for (a)–(f), respectively) in the 3370–3470-$cm^{-1}$ region, showing the internal rotation subbands. (g) is the same region for the $n$ = 8 cluster which does not show the internal rotation structure. (Due to poor signal to noise, a larger wavelength increment was used in (g) than the scans in (a)–(f), but averaging time was increased.) The notation is discussed in the text. Corresponding subbands are connected by solid lines.

the rotational motion of the methyls through the 3-fold potential barrier is analyzed, taking into account the torsional barrier height, the degree of vibration–vibration coupling in the system, and the difference between upper and lower state rotational constants of the molecule. By use of this approach, the $\nu_9$, $\nu_{13}$ band is reproduced to nearly the limit of experimental resolution. For 2-butyne, it was found that the barrier to internal rotation was small, less than 10 $cm^{-1}$.[41-44] Microwave spectra later demonstrated that the barrier to internal rotation was 5.6 $cm^{-1}$.[45]

(44) Mills, I. M.; Thompson, H. W. *Proc. R. Soc. London, Ser. A* **1954**, *226*, 306.
(45) Nakagawa, J.; Hayashi, M.; Endo, Y.; Saito, S.; Hirota, E. *J. Chem. Phys.* **1984**, *80*, 5922.

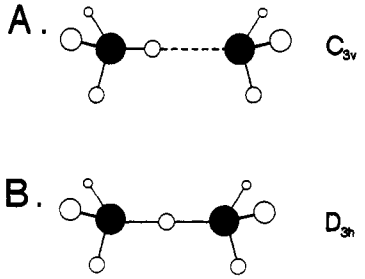


**Figure 7.** $C_{3v}$ and $D_{3h}$ equilibrium structures for $N_2H_7^+$. The energies are expected to differ by only a few kcal/mol, with the relative energy ordering uncertain.

Exploiting the similarity between 2-butyne and the symmetric form of the $N_2H_7^+$ cluster ion, we have used the same formalism outlined by Papousek to simulate the antisymmetric stretching band, $\nu_3$. For an ethane-like molecule, Papousek derived the expression for the fundamental band of a perpendicular transition involving $E_{1d}$ and $E_{2d}$ species. Frequencies for the fine structure transitions involved in the rotational Q branches of a transition from the ground vibrational state are given by the following:

$$\nu + \theta + \{A'(1 - 2\zeta_r^z) - B'\} \bullet 2[A'(1 - \zeta_r^z) - B']K \pm E(K_i)$$

where

$$\theta = [(A' - A'') + (B'' - B')]K^2 + (A' - A'')K_i^2 + (B_i' - B'')J(J + 1)$$

$$E(K_i) = 2A'(1 - \zeta_r^z)K_i + \Delta_v^2/[16A'K_i(\zeta_r^z - 1)]$$

In these expressions, the vibrational band origin is denoted by $\nu$. $A$ and $B$ are the rotational constants of the molecule, and the single and double primes denote the excited- and ground-state constants, respectively. $K$ and $J$ are the usual rotational quantum numbers of the molecule. $K_i$ is the torsional quantum number for internal rotation, and $B_i$ is the rotational constant of one of the rotating subgroups around its local $C_3$ axis. $\zeta_r^z$ and $\Delta v$ are the Coriolis coupling term and the vibration–vibration coupling term, respectively. Terms with the upper sign hold for $\Delta K = +1$ and the lower for $\Delta K = -1$. For transitions from single-valued states, the quantum numbers $K$ and $K_i$ have the same parity; for transitions from the double-valued states, the opposite parity.

The perpendicular transition to the $E_{1d}$ state should follow the selection rules $\Delta J = 0, \pm 1$, $\Delta k = \pm 1$ ($K = |k|$), and $\Delta k_i = 0$ ($K_i = |k_i|$). More details may be found in refs 41 and 42.

In Figure 8a, a simulated spectrum calculated by using the above expressions for $K = 0$ to $\pm 1$, $K_i = -9$ to $+9$, and $J = K$ to $K + 9$ is shown. The relative intensities of the lines in the spectrum are calculated from the Boltzmann factors, statistical weights of nuclear spin states, and orientation factors of the ground vibrational state. A Lorenzian convolution of the line spectrum so generated is employed with a fwhm of 1.0 $cm^{-1}$ to simulate the resolution of the machine function.

For this simulation the only parameters that were systematically varied were the vibrational band origin of the transition, $\nu$, the rotational temperature of the molecule, and the vibration–vibration coupling constant $\Delta v$. Values for the $A'$ and $B'$ rotational constants were selected assuming a symmetric structure. The excited-state vibrational constant $A''$ was set at 3.16 $cm^{-1}$, and $B''$ was set equal to $B'$. The coriolis coupling constant and the torsional barrier height were both neglected. Values for the constants used appear in the figure caption.

One can see that, in spite of the fact that the calculated spectrum does not include R- and P-branch structure, there is reasonable agreement with the experimental results in Figure 8b for the major features. Unfortunately, the shoulders present to the blue of the Q-branch maxima are not reproduced. For the $^RQ_K$ series in a symmetric top, the R branch can be somewhat more intense than the P branch. Thus, the weak feature at 3402 $cm^{-1}$ may be attributable to an R branch of $^RQ_0$, as it peaks in the correct position for the expected rotational temperature of ≈20 K and a rotational constant of 0.3 $cm^{-1}$.

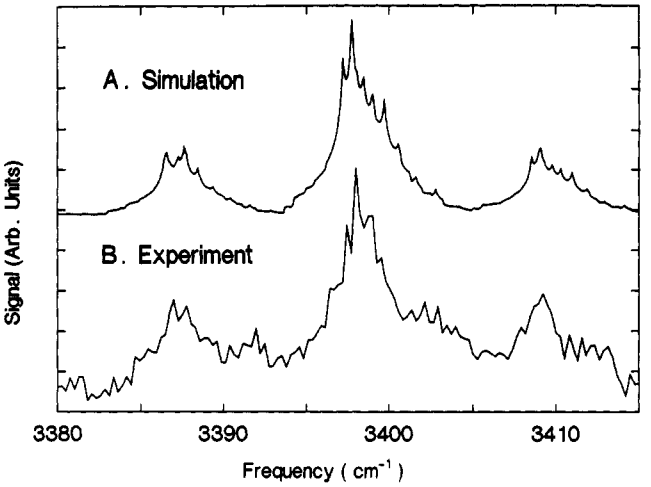


**Figure 8.** Simulated and experimental spectrum of $N_2H_7^+$ for $D_{3h}$ equilibrium structure of Figure 7b. The simulation includes only Q-branch transitions, since these are expected to dominate the spectrum. While the two traces show similarities, there are substantial differences as well. Rotational constants used in the simulation are as follows: $A'$ = 3.20 $cm^{-1}$, $A''$ = 3.16 $cm^{-1}$, $B' = B''$ = 0.16 $cm^{-1}$, $T$ = 30 K, $_\Delta V = -1.0$, $\zeta$ = 0.0.

There is certainly a possibility that these features might be due to hot bands. A more likely explanation would be that this anomalous structure involves a rotation of the entire $NH_3$–$H^+$–$NH_3$ ion about its $C_3$ axis rather than just one $NH_3$ subunit about its local axis. As stated earlier, this structure would have half the spacing of the internal rotation structure and could lead to peaks located roughly halfway between the internal rotation Q branches. Such issues can be resolved by more detailed studies at higher spectral resolution which are presently under way.

The simulation seems successful in that the relatively large splitting in the $\Delta K = 0$ and $\Delta K = -1$ subbands are reproduced, as is the smaller splitting in the $\Delta K = +1$ subband. This splitting arises in the simulation through the introduction of a small amount of vibration–vibration coupling into the energy expression through the $\Delta v$ constant. The fact that the fit obtained for this spectrum did not require recourse to the formalism for a torsional barrier suggests, as in the case of 2-butyne, that the internal rotation is nearly free. That this should be the case is not entirely obvious from the standpoint of molecular geometries. In 2-butyne the distance between the hydrogens on different methyl substituents is about 4.9 Å. This distance is about 3.4 Å for the ab initio[12] structure $NH_4^+(NH_3)$ (about 0.2 Å less for the symmetric structure). The N–N distance in this ion is comparable to the N–C distance in the T-shaped van der Waals complex $NH_3$–$CO_2$, which also has a low barrier to internal rotation of less than 14 cal/mol.[46] From the relatively successful modeling of the spectrum in the same way as dimethylacetylene (see Figure 8) and the strong dependence of the appearance of the internal rotation bands on the torsional barrier height, we conclude that an upper limit to the torsional barrier height can be placed at about 10 $cm^{-1}$. In order to apply this theory to the larger clusters, it must be adapted for the particular geometry and the complete nuclear permutation inversion (CNPI) group.

The frequency of the central $^RQ_0$ band for $n = 1$ as compared to $n > 1$ (these will be compared later) and the absence of two bands of comparable intensity (one each for "$NH_4^+$" and "$NH_3$" groups) suggest that, contrary to the ab initio results, the equilibrium structure of $N_2H_7^+$ is the symmetric one. With this configuration, the cluster would best be described by the formula $H_3N{\cdot}H^+{\cdot}NH_3$ rather than $NH_4^+{\cdot}NH_3$. It should be possible to determine the structure conclusively when a $H_2$ messenger study is performed as in the case of $H_5O_2^+$ and/or the spectrum is recorded at sufficiently high resolution to determine the rotational constant $B = C$. The rotational constant will allow an estimation

(46) Fraser, G. T.; Leopold, K. R.; Klemperer, W. *J. Chem. Phys.* **1984**, *81*, 2577.

of the N–N separation, which in turn should indicate whether the proton is equally shared by the nitrogens.

For the $H_5O_2^+$ system studied previously by a "messenger" technique, the small perturbation by a $H_2$ molecule on the $H_5O_2^+$ cluster is thought to lead to the formation of an asymmetric structure involving species similar to $H_3O^+$ and $H_2O$.[47,48] Since the isolated $H_5O_2^+$ species is best thought of as $H_2O{\cdot}H^+{\cdot}OH_2$ rather than $H_3O^+{\cdot}OH_2$, the presence of the weakly bound "messenger" led to a dramatically different spectrum, providing qualitative confirmation that the isolated $H_5O_2^+$ has a symmetric equilibrium structure. The definitive confirmation, of course, will probably come from a determination of the much lower vibrational frequencies involving the hydrogen-bonded proton, as these are very sensitive to the structure.

*2. $NH_4^+(NH_3)_2$.* The spectrum for the $NH_4^+(NH_3)_2$ cluster ion appears in Figure 6b. With a $\Delta H°$ of solvation of 17.5 kcal/mol for the $n = 1 \rightarrow n = 2$ clustering step,[7] this cluster is too strongly bound for two photons of 3000-$cm^{-1}$ light to easily predissociate a solvent molecule unless a significant amount of internal excitation is already present. As in the case of the $n = 1$ cluster, the two-color excitation scheme was used to study this system.

Ab initio calculations for the structure of the $n = 2$ cluster by Hirao et al.[12] predict that the cluster should have the $C_{2v}$ symmetry assumed by Schwarz. Alignment of the solvent ammonias along two of the four available binding sites in the first solvation shell yields an ammonium ion whose stretching vibrations can be roughly divided into two categories: hydrogen bonded and non-hydrogen bonded. In the bonded category we have a symmetric and an antisymmetric mode, each involving the solvated core N–H bonds and appearing at relatively low frequency. In the nonbonded category we have a symmetric and an antisymmetric mode, each involving the unsolvated core N–H bonds and appearing at relatively high frequency. For the $NH_3$ solvent molecules, a symmetric stretch ($\nu_1$) and a doubly degenerate antisymmetric stretch ($\nu_3$) are expected; these involve the three free N–H bonds of the $NH_3$ subunit (see Figure 5). For this study, we will consider the vibrational bands of equivalent subunits in the complex to be degenerate for all ammoniated ammonium complexes.

Schwarz observed two broad peaks that he assigned to transitions involving modes of the $NH_4^+$ ion. A broad feature was observed in the 2400–2600-$cm^{-1}$ region which was tentatively assigned to the low-frequency N–H stretches, and a relatively narrow unidentified peak was observed at 2280 $cm^{-1}$. This latter peak we suspect may actually be the symmetric stretch of the two bound N–H oscillators. A higher frequency feature at 3360 $cm^{-1}$ was assigned to the two free N–H stretches.

In this work, the low-frequency peak lies below the lowest frequency accessible to the present laser system, but a series of transitions in the 3400-$cm^{-1}$ region are observed. Shown in Figure 6b, Schwarz's peak around 3360 $cm^{-1}$ is resolved into two main bands. The first, which seems to be split into two maxima at 3392 and 3395 $cm^{-1}$, is assigned to the antisymmetric N–H stretches of the two free N–H oscillators of the ammonium core. Under the notational scheme discussed earlier, these bands would be designated $^20°$ $N\text{–}H^{fr}_{astr}$.

The symmetric stretch of these N–H bonds was not observed. This is not particularly surprising as it has been observed previously that the symmetric stretch of complexed ammonia has a particularly low infrared transition dipole moment.[49]

A series of subbands is present slightly to the blue, with similar structure as the feature in the $n = 1$ spectrum, and has been assigned to the $\nu_3$ band of the ammonia solvent molecules. Under our new notation we would designate this band as $^21°$ $N\text{–}H^{fr}_{astr}$. With $^RQ_0$ at 3413.7 $cm^{-1}$ and an average spacing between adjacent components of 12.6 ± 0.3 $cm^{-1}$, this structure is again due to internal rotation of the ammonia subgroups. For this cluster, where the perturbation of the $NH_3$ solvent molecules is less, the subband spacing agrees very well with the 12 $cm^{-1}$ expected for free ammonia rotation about its $C_3$ axis. If the assignment of the $\nu_3$ subbands is correct with respect to $K$, then this band falls nicely into the progression established by $n = 1$ and $n = 3$–7. (We will discuss this series in more detail later.) However, this assignment appears to have some intensity anomalies; $^PQ_1$, for example, appears much more intense than $^RQ_1$. While this anomaly could possibly be due to an experimental artifact, one possible explanation is that the $\nu_3$ state of the $NH_3$ subunits somehow interacts with the antisymmetric stretch of the free N–H oscillators of the core. Since the upper state of $^PQ_1$ is about 25 $cm^{-1}$ closer to this state than that of the upper level of $^RQ_1$, $^PQ_1$ is in a position to borrow more intensity. However, it is not clear why these levels should interact, and there is no corresponding frequency anomaly. A more attractive explanation is that the core antisymmetric stretching band is actually quite broad, 15–20 $cm^{-1}$, and therefore the intensity of $^PQ_1$ appears large because it resides on the shoulder of this band. We therefore take $^RQ_0$ at 3414 $cm^{-1}$ as the most likely assignment.

*3. $NH_4^+(NH_3)_3$.* The spectrum for the $n = 3$ ammoniated ammonium ion appears in Figures 6c and 9a. The expected geometry should have roughly $C_{3v}$ symmetry with the solvent molecules associating with three of the hydrogens on the central ammonium ion. Schwarz analyzed the vibrations for the $NH_4^+$ core under these conditions in terms of distorted $T_d$ symmetry. Under this framework, six fundamentals are expected for the core, all infrared active. Of these, those that might be of a high enough frequency for the present laser system to excite are the stretching motions of the core: $\nu_1'$, characterized primarily by the symmetric stretch of the hydrogen-bonded core N–H's; $\nu_3'$, the antisymmetric stretch involving the free N–H bond; and $\nu_3''$, the antisymmetric stretch involving the hydrogen-bonded N–H's. Of these, $\nu_3'$ should appear at a higher frequency than either $\nu_1'$ or $\nu_3''$, which should have roughly the same frequency. One would also expect to observe transitions involving the solvent $NH_3$'s.

In Figure 9a, two strong absorptions are observed at 2660 and 2692 $cm^{-1}$, in agreement with Schwarz's low-resolution observation of a single strong peak at 2682 $cm^{-1}$. Labeled with a B in Figure 9a, these could be assigned to the fundamentals of the $\nu_1'$ and $\nu_3''$ vibrations discussed above. An alternative and somewhat more plausible assignment is that these two peaks, which are of equal intensity, arise from lifting the degeneracy of the $\nu_3''$ doubly degenerate mode. The small peak at 2615 $cm^{-1}$ is then taken to be $\nu_1'$. Of course, a high-quality ab initio calculation of the intensities may be able to indicate which assignment is correct.

It is interesting to note that our spectrum of $n = 3$ shows a very broad background absorption in the 2600–3100-$cm^{-1}$ region which is so nearly featureless it is almost a continuum at our level of spectral resolution. When the spectrum was taken with a decreased backing pressure behind the nozzle resulting in a rotationally warmer expansion, the peaks broadened very much and the "continuum" became much more prominent relative to these peaks. A glance at Schwarz's $n = 3$ spectrum indicates that the absorption is more intense in the 400-$cm^{-1}$ region to the blue of the intense 2680-$cm^{-1}$ peak than 400 $cm^{-1}$ to the red, although in each case there is measurable absorption for the entire 400-$cm^{-1}$ expanse. It will be seen later that the spectra of all the larger clusters show some absorption in the region above the ion core hydrogen-bonded N–H stretches. We believe this to result from hot bands and combination bands involving these stretches and those of the hydrogen bonds themselves. The latter might be expected to have frequencies of 50–400 $cm^{-1}$ for $n = 2$–10, with the largest frequencies associated with the smallest values of $n$.

The free N–H stretching vibration $\nu_3'$ appears at 3374 $cm^{-1}$, again near the 3365 $cm^{-1}$ measured by Schwarz. Also observed is the antisymmetric stretch of the solvent $NH_3$'s centered at 3416.8 $cm^{-1}$ with the internal rotation structure observed previously. (See Figure 6c for an expanded view of this region.) An inspection of the intensities of the Q branches shows some enhancement in the $K = \pm 3$ stacks, consistent with the spin statistics

(47) Okumura, M.; Yeh, L. I.-C.; Lee, Y. T. *J. Chem. Phys.* **1985**, *83*, 3705.

(48) Okumura, M.; Yeh, L. I.-C.; Meyers, J. D.; Lee, Y. T. *J. Chem. Phys.* **1986**, *85*, 2328.

(49) Pimentel, G. C.; Bulanin, M. O.; Van Theil, M. *J. Chem. Phys.* **1962**, *36*, 500.

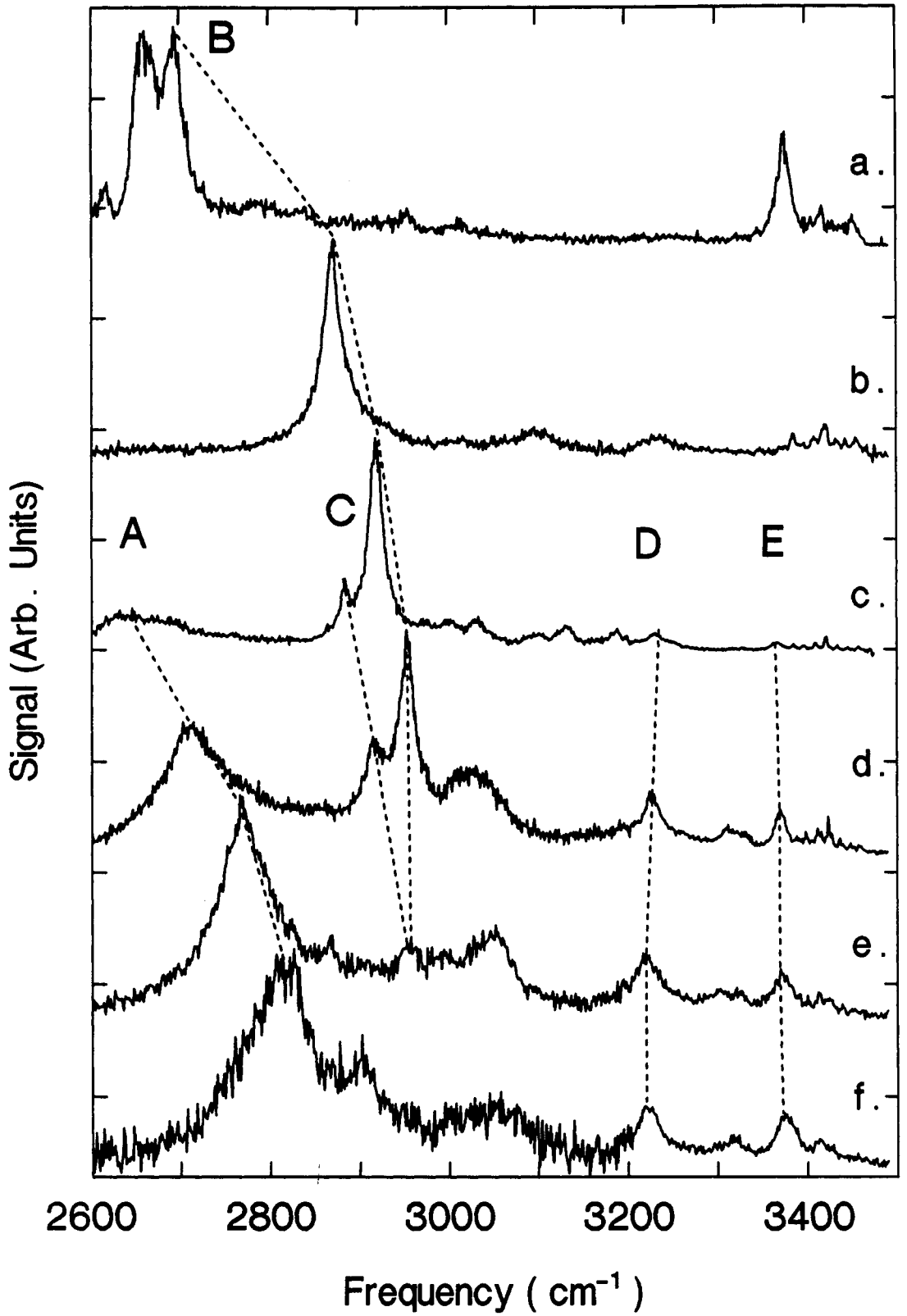


**Figure 9.** Vibrational predissociation spectra of $NH_4^+(NH_3)_n$ ($n$ = 3-8 for (a)-(f), respectively) in the 2600-3500-cm$^{-1}$ region. Bands forming clear series in $n$ are connected by dashed lines.

expected for an ammonia rotating about its $C_3$ axis.

*4. $NH_4^+(NH_3)_4$.* Thermodynamic measurements and theoretical structural calculations indicate that the $n$ = 4 cluster ion represents the completion of the first solvation shell of the $NH_4^+$ ion. With four degenerate $NH_3$ solvent molecules, the cluster has the same $T_d$ symmetry as the isolated ion core species[14,15] (see Figure 10a). Therefore, only two fundamentals of the core should be infrared active: $\nu_3$, the triply degenerate antisymmetric stretch, and $\nu_4$, the doubly degenerate bending mode.

In the survey spectrum reported previously[17] (see Figure 9b), four main features are observed. The most prominent feature was assigned by Schwarz to the fundamental of the $\nu_3$ vibration. The value from the present work of 2865 cm$^{-1}$ agrees well with Schwarz's measurement of 2867 cm$^{-1}$ for the position of this band. This band is connected to the analogous core vibration in the $n$ = 3 spectrum with a dashed line labeled B in the figure.

Although the doubly degenerate $\nu_4$ bending mode occurs at too low a frequency for either Schwarz or the present workers to

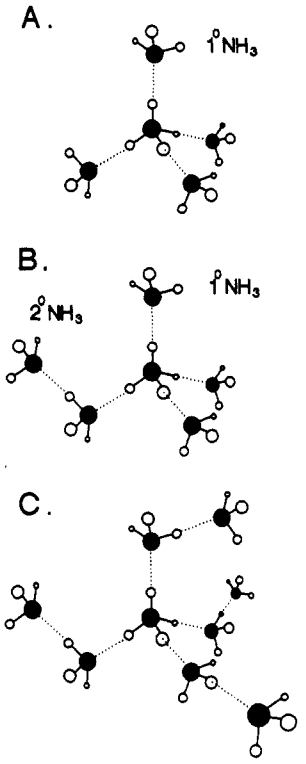


**Figure 10.** Proposed structures for the $n = 4$, 5, and 8 complexes. The hydrogen bonds are denoted by dashed lines. It is not certain that the hydrogen bonding between 1° and 2° $NH_3$ is linear.

measure (1400 $cm^{-1}$ in matrices), Schwarz was able to observe the first overtone of the bending mode, $2\nu_4$, at 3087 $cm^{-1}$. This assignment was supported by an isotope substitution study in which a comparison of the Teller–Redlich product ratio[50] for the antisymmetric stretch and the bending overtones in $NH_4^+$, $ND_4^+$ and $CH_4$, $CD_4$ was made. In the present work, the $2\nu_4$ band is observed at 3095 $cm^{-1}$. Other bands are evident in the survey spectrum that have been assigned to modes of the solvent $NH_3$'s.

As in the previous spectra, the antisymmetric stretching vibration of the first solvent shell ammonias is observed, centered at 3419.5 $cm^{-1}$ with the structure due to internal rotation (see Figure 6d). With an average separation of 12.3 $cm^{-1}$ between adjacent components, this band can be well fit to a model in which a single ammonia molecule is rotating freely about its $C_3$ axis attached to a "wall". In fact, the appearance of all the $\nu_3$ bands for $n = 3$–6 is very similar, so that all of them could be reasonably fit at the present resolution by the same model. By use of a simple symmetric top expression for the position of the Q branches, and the Hönl–London expressions for the transition intensities, this band has been fit to a rotational temperature of 35 K with respect to the $K$ quantum number. The strong–weak–weak–strong intensity alternation expected for a molecule with $C_{3v}$ symmetry is easily observed here. Intensities of subbands originating from $K = 0$ and $K = 3$ ($^RQ_0$, $^PQ_3$, and $^RQ_3$ in the figure) have about twice the intensity expected from the calculation just mentioned if nuclear spin statistics are not considered.

A second transition of the solvent molecules appears at approximately 3230 $cm^{-1}$ and has been tentatively assigned to $2\nu_4$, the first overtone of the $\nu_4$ bending mode. It is marked by a dashed line labeled D in Figure 9b. There is a small possibility that the $\nu_1$ symmetric stretching band overlaps with $2\nu_4$, but this is unlikely because it would require a much larger shift of the symmetric stretch in $NH_3$ upon complexation compared to that of the antisymmetric stretch, 100 $cm^{-1}$ vs 30 $cm^{-1}$. Since the complexation of $NH_3$ generally results in a reduction of $\nu_1$ intensity relative to $\nu_3$,[51] we believe that the $\nu_1$ absorption is very weak and was consequently unobserved for $n = 4$.

The disappearance of the 3374-$cm^{-1}$ band in the $n = 3$ spectrum, which was assigned to the free N–H stretching motion of the core oscillator not bound by a solvent molecule, shows that the fourth solvent $NH_3$ indeed occupies the last first shell site on the $NH_4^+$ ion.

*5. $NH_4^+(NH_3)_5$.* All of the thermodynamic and ab initio data are in agreement that the first solvent shell is filled at $n = 4$. The ab initio calculation of Hirao et al.[12] predicts that the fifth $NH_3$ hydrogen bonds to one NH oscillator of a 1° $NH_3$. The spectrum of $n = 5$ shows conclusively that this is correct. There is strong support for this picture of the binding that leads to the weakening of one core NH oscillator and strengthening of the other three.

The $NH_3$ attached to the first solvation shell alters both spectral features associated with the $NH_4^+$ ion core of the cluster and the first solvation shell (1°) ammonia that this second solvation shell (2°) $NH_3$ is bound to. For the $n = 4$ cluster, the $\nu_1$ symmetric stretching vibration is not infrared active due to the $T_d$ symmetry of the environment around the core and the core itself. By addition of another $NH_3$ outside the first shell, this motion should become weakly IR active. Similarly, the triply degenerate antisymmetric stretch of the core, $\nu_3$, will split into a doubly degenerate antisymmetric stretching component of higher frequency, $\nu_3'$, similar to that for the $n = 4$ cluster, and a lower frequency component, $\nu_3''$, dominated by the N–H stretching motion of the core bound to both a 1° and a 2° $NH_3$.

In the spectrum shown in Figure 9c for the $n = 5$ cluster, the small, sharp feature observed at 2890 $cm^{-1}$ and labeled C is assigned to the symmetric stretching motion of the core, $\nu_1'$. The weak intensity of this band is consistent with the only slight breaking of the symmetry of the core by the 2° ammonia.

Another new, broad feature centered at 2650 $cm^{-1}$, labeled A in the figure, is correlated with the addition of an $NH_3$ into the second solvation shell. The fact that this feature greatly increases in relative intensity as the number of solvent molecules increases beyond $n = 5$ (see the following section) lends support to the notion that it involves a vibration coupled to the second solvation shell ammonias. We assign it to the low-frequency component of the antisymmetric stretch of the core, $\nu_3''$. The large width of the feature (50–60 $cm^{-1}$ fwhm) even at the low rotational temperatures of this study suggests that extensive hydrogen bonding is involved. The intense 2910-$cm^{-1}$ band, B, also associated with an oscillator involved in hydrogen bonding, is relatively narrow (25 $cm^{-1}$ fwhm). This peak can be clearly assigned to $\nu_3'$. The smaller width of this band, even when compared to $\nu_3$ in $NH_4^+(NH_3)_4$, correlates with the strength of the hydrogen-bonding interaction.

A series of weak absorptions appear in the 3000–3200-$cm^{-1}$ region. The group of two peaks centered at 3010 $cm^{-1}$ and an additional set of two peaks centered at 3110 $cm^{-1}$ probably correlate to the features in the $n = 4$ spectrum at 3010 and 3095 $cm^{-1}$ respectively. There, the identity of the first feature was uncertain, and there was strong evidence from Schwarz that the second was due to the first overtone, $2\nu_4$, of the triply degenerate bending mode of the core. On the basis of the latter identification, we tentatively assign the 3110-$cm^{-1}$ group to a similar bending motion. Because of the loss of degeneracy produced by the second shell ammonia, the bending mode can be expected to split into a high-frequency and a low-frequency component, the lower of which would probably be most closely associated with the three equivalent core oscillators. A splitting of 30 $cm^{-1}$, as observed, does not seem unreasonable. The 3010-$cm^{-1}$ set of peaks is presumably an overtone or combination band. One possibility is a combination of the $\nu_1'$ and intense $\nu_3'$ modes (2890- and 2910-$cm^{-1}$ peaks) with the intense low-frequency hydrogen-bond stretching modes. This would place the stretching frequency of the three equivalent hydrogen bonds at about 110 $cm^{-1}$, which also does not seem unreasonable. Another possibility is that these peaks are due to a bending overtone of the core oscillator with attached 1° and 2° $NH_3$ ligands. In this case, the 3110-$cm^{-1}$ group would be assigned

(50) Herzberg, G. *Infrared and Raman Spectra of Polyatomic Molecules*; D. Van Nostrand: New York, 1945; pp 231, 307.

(51) Pimentel, G. C.; Bulanin, M. O.; Van Thiel, M. *J. Chem. Phys.* **1962**, *36*.

to the bending overtone of the other three oscillators.

The addition of an $NH_3$ into the second shell should also have an effect on the 1° ammonia to which it attaches. If the bonding occurs through the sort of hydrogen bond illustrated in Figure 10b, one would expect the 12-$cm^{-1}$ characteristic spacing of free internal rotation of 1° $NH_3$ to disappear when the 1° $NH_3$ is bound to a 2° $NH_3$. The antisymmetric stretching motion of the 1° solvent molecule would also be split into a low-frequency hydrogen bound component and two higher frequency free N–H stretching motions: a symmetric stretching component and an antisymmetric one.

Centered at 3419.8 $cm^{-1}$ and shown in expanded view in Figure 6e is the now familiar structure due to internal rotation of the 1° $NH_3$'s superimposed on the antisymmetric stretching vibration of the subgroups. Band "E" in Figure 9c, at 3364 $cm^{-1}$, however, is a new feature not observed for $n$ = 4 and arises from the presence of the 2° $NH_3$. The frequency is appropriate for NH oscillators which are not hydrogen bonded. This band is significantly broader than the individual components of the $NH_3$ $\nu_3$ band and shows no rotational structure at this level of resolution. It is assigned to the free N–H antisymmetric stretching motion of the 1° $NH_3$ bound to the 2° $NH_3$, denoted $^21°$ N–$H^{fr}_{astr}$ in the new notation.

The band labeled D in Figure 9c centered at 3230 $cm^{-1}$ has gained considerably in intensity from $n$ = 4 to $n$ = 5. We assign this feature to two overlapping bands, one due to the bound N–H oscillator of the 1° $NH_3$, $^11°$ N–$H^{bd}_{str}$. The other band is due to $2\nu_4$ of the three equivalent unbound 1° $NH_3$ subunits, although the remaining 1° $NH_3$ and the 2° $NH_3$ may also contribute intensity by N–H bending overtones. By $n$ = 6, we certainly expect the majority of intensity in the solvent region of the spectrum to come from the N–H stretch of 1° hydrogen-bonded oscillators, although we cannot rule out significant contribution from bending overtones. Once again, ab initio calculation might help to clarify this. It seems, however, that the structure of $n$ = 5 is of the sort given in Figure 10b. It is also clear due to the lack of the 3370-$cm^{-1}$ feature found in the $n$ = 5–8 spectra that in the $n$ = 4 spectrum there is essentially no $n$ = 4 isomer with a 1°–2° $NH_3$ hydrogen bond.

The contribution of the outer shell $NH_3$ N–H oscillators to the $n$ = 5 spectrum is minor and could not be identified. When the $n$ = 8 spectrum is discussed later, however, it will be suggested that the barrier to internal rotation is higher for outer $NH_3$ subunits in $n$ = 5–8 complexes than for nonbonded 1° $NH_3$ in $n$ = 1–7 complexes.

*6. $NH_4^+(NH_3)_6$.* As the number of solvent molecules around the $NH_4^+$ increases, the production of isoenergetic conformers becomes more likely. A consequence of this is that speculations about the detailed structure of the larger ammoniated ammonium ions becomes less certain. However, it seems reasonable to suppose that the structure of the first solvation shell is reasonably well-preserved and that the addition of subsequent ammonias tends to occur predominantly through the sort of hydrogen-bonding scheme discussed in the previous section. The spectra are found to be consistent with this assumption.

Working from the premise that additional solvent molecules bind to successive first shell ammonias, we presume that by the $n$ = 6 cluster two of the four available second shell sites are occupied. Using the $n$ = 5 cluster as a model for the spectrum, we would expect the components of the core vibrational band assigned to a stretching motion where N–H bonds of the core are bound to both a 1° and a 2° $NH_3$ ($^20°$ N–$H^{bd,bd}_{str}$) to increase in relative intensity. Conversely, the feature associated with the antisymmetric stretch of the core bound only to 1° ammonias should decrease in relative intensity ($^20°$ N–$H^{bd}_{astr}$).

A glance at Figure 9d shows that this is the case, as peak A increases dramatically in intensity relative to peak B. Recall that peak A was first observed in the $n$ = 5 spectrum and is therefore associated with the onset of the second solvation shell. In addition to a sharp increase in intensity, it has also shifted to higher frequency, 2720 $cm^{-1}$. Again, this band is assigned to a stretching motion of the core where the N–H bonds involved are themselves bound to both a 1° and a 2° $NH_3$ ($^20°$ N–$H^{bd}_{astr}$). We call it an antisymmetric stretch because symmetric stretches, in general, seem to carry less intensity. At 2920 $cm^{-1}$, the symmetric stretching motion of the core oscillators bound to only 1° ligands is observed ($^20°$ N–$H^{bd}_{sstr}$) and is labeled C in Figure 9d. The antisymmetric stretching motion of the same core oscillators, $^20°$ N–$H^{bd}_{astr}$, is observed at 2950 $cm^{-1}$ and labeled B. A broad band whose maximum occurs at 3020 $cm^{-1}$ is observed and is tentatively assigned to the first overtone of the overlapping core bending modes $^20°$ N–$H^{bd,bd}_{bend}$ and $^20°$ N–$H^{bd}_{bend}$, with a possible contribution from a combination band involving $^20°$ N–$H^{bd}_{str}$ and the hydrogen-bond stretch.

The effect of further occupation of the second solvation shell should also have an effect on the spectroscopy of the first solvation shell ammonias. The structure due to internal rotation of the 1° solvent molecules is still observed, but at much lower relative intensity. With $^RQ_0$ centered at 3422 $cm^{-1}$, this structure lies slightly to the blue of the analogous $n$ = 4 and 5 bands (see Figure 6f). The structure assigned to the free N–H antisymmetric stretching motion of the 1° ammonias bound by the second solvation shell ammonias $^21°$ N–$H^{fr}_{astr}$, E in Figure 9d, has greatly increased in relative intensity and appears at 3368 $cm^{-1}$. Similarly, the $^11°$ N–$H^{bd}_{sstr}$ mode has increased in intensity and appears at 3225 $cm^{-1}$. This feature is labeled D.

The weak feature at about 3320 $cm^{-1}$ is probably the symmetric stretch $\nu_1$ of the two 2° ammonias, overlapped with the symmetric stretch of free N–H oscillators of those 1° subunits with an attached 2° $NH_3$. There is a slight indication that a very weak band is present here in the $n$ = 5 spectrum as well. While the $\nu_1$ and $\nu_3$ bands in isolated $NH_3$ have comparable intensity, it has been clear that in the complexes $n$ = 1–5 the $\nu_3$ band of $NH_3$ subunits carries much more intensity than $\nu_1$. The appearance of $\nu_1$ at $n$ = 6 with comparable intensity to $\nu_3$ could then be taken as an indication of how weakly the second shell $NH_3$ subunits are bound. The 3320-$cm^{-1}$ band, upon close inspection, seems to consist of two peaks at 3310 and 3325 $cm^{-1}$. A careful comparison of the $n$ = 7 spectrum in the same region reveals similar structure. By analogy with the symmetric stretch observed in the spectrum of liquid ammonia[52] at 3300 $cm^{-1}$ and similar structure observed in clusters of neutral ammonia clusters,[53] we tentatively assign the 3310-$cm^{-1}$ peak to the symmetric stretch of primary subunits, $^21°$ N–$H^{bd}_{sstr}$. By analogy to $\nu_1$ in isolated $NH_3$, we tentatively assign the 3325-$cm^{-1}$ peak to $\nu_1$ of the two second shell ammonias. The two remaining first shell unbound ammonias are presumed to constitute a minor contribution.

*7. $NH_4^+(NH_3)_7$.* It is obvious how most of the $n$ = 7 features in Figure 9e correlate with $n$ = 6 in Figure 9d. Most of the difference in appearance of the two spectra has to do with the modes of the $NH_4^+$ core at frequencies below 3100 $cm^{-1}$. It is very obvious that the intense 2770-$cm^{-1}$ peak of $n$ = 7, A in the figure, correlates with the 2720-$cm^{-1}$ peak of $n$ = 6 (it will be shown later that the two peaks fall into a smooth frequency progression established by the other clusters), and we readily assign it as $^30°$ N–$H^{bd,bd}_{astr}$. The fwhm of the band is about 80 $cm^{-1}$, slightly less than for the analogous band in $n$ = 6. This reduction is consistent with the lower hydrogen-bond strength in $n$ = 7. The intense 2950-$cm^{-1}$ peak in $n$ = 6 and its companion at 2920 $cm^{-1}$ (B and C in Figure 9d) have nearly disappeared in the $n$ = 7 spectrum. It is expected from our $n$ = 6 assignments that these two peaks should collapse into one peak of reduced intensity for $n$ = 7, if the cluster consists of an $NH_4^+$ core, four first shell $NH_3$ subunits, and three second shell $NH_3$ subunits, each hydrogen-bonded to its own primary subunit. In fact, it appears that the peaks do collapse, and the reduction in intensity is surprisingly dramatic. In the spectra of the higher ammoniates, such a peak is not observed, suggesting that all of the N–H bonds of the ammonium core are experiencing hydrogen bonding with both 1° and 2° solvent molecules.

(52) Bertran, J. F. *J. Mol. Struct.* **1982**, *95*, 9. Corset, J.; Lascombe, J. *J. Chem. Phys.* **1967**, *64*, 665.

(53) Vernon, M. Ph.D. Thesis, University of California, Berkeley, 1982.

The only new feature appears at 2870 $cm^{-1}$ and is quite weak. This band is more prominent in the $n = 8$ spectrum. Our very tentative assignment is to a combination band involving the core stretching mode $^{3}0°$ $N\text{-}H_{astr}^{bd,bd}$ and the hydrogen bond to these three equivalent oscillators. If correct, this assignment places the frequency of this strongest of the hydrogen bonds in $n = 7$ at about 70–90 $cm^{-1}$.

The band centered at 3050 $cm^{-1}$ seems to be a bending overtone of the three equivalent N–H oscillators. The remaining features at 3020 and 2990 $cm^{-1}$ might be produced by bending overtones of other N–H oscillators.

From the above discussion, it seems that the lowest energy structure consists of an $NH_4^+$ core with four 1° $NH_3$ ligands and three 2° $NH_3$ ligands, each attached to a different 1° subunit. There is no definitive indication for the symmetric structure $(NH_3)_3(N_2H_7^+)(NH_3)_3$, analogous to the species $(H_2O)_2$-$(H_5O_2^+)(H_2O)_2$ which is proposed to be an intermediate in proton transfer,[29] nor any other isomer. There is also no strong indication for a "cross-linking" of second shell ammonia to another ammonia subunit in the first or second shell, with the formation of large ring structures. It is clear from the $\nu_3'$ band of the propellering first shell $NH_3$ that this subunit is not involved in cross-linking. If there is cross-linking of two second shell ammonias, however, it may be difficult to discern from the spectrum due to the weak absorptions of these subunits and the possibility that the absorptions may overlap with those of primary ammonia.

*8. $NH_4^+(NH_3)_{8-10}$.* One would expect that as the number of $NH_3$ molecules around the $NH_4^+$ increases, the spectrum of the ammoniated ammonium ion cluster should eventually converge. In the limiting case, this spectrum would be that of an ammonium ion solvated in a liquid ammonia environment. Spectral features associated with an ammonium ion bound to both 1° and 2° ammonias should further increase in relative intensity. Conversely, $NH_4^+$ stretches involved in bonding to 1° $NH_3$'s only should disappear at $n = 8$ provided that the second shell, like the first shell, is filled by four ligands, each bound to a separate primary ammonia. For the 1° $NH_3$ molecules, free rotation as observed in the $n = 1$–6 spectra should be quenched for $n > 7$. A similar band structure could take its place, but associated with 2° $NH_3$. Absorptions due to second and third shell ammonia might be very apparent by $n = 10$. Stretching vibrations of the solvent subunits should begin to approach those observed in the condensed phases. Unfortunately, spectra for the $n = 9$ and 10 clusters were limited by low signal-to-noise ratio to the 2600–3200-$cm^{-1}$ region because of the weak absorbance in the higher frequency region and the low number density of larger mass clusters obtainable.

The IRVPD spectra for the $n = 8$ ammoniated ammonium ion cluster appear in Figures 6g and 9f. For the higher ammoniates, the spectra are essentially the same as that of the $n = 8$ species. Band maxima for the features observed in the $n = 8$–10 spectra are listed in Table III.

Once again, the assignments stem from those of the smaller clusters. The very intense peak at 2830 $cm^{-1}$, A, is an antisymmetric stretch of the core N–H oscillators, which is analogous to the triply degenerate $\nu_3$ fundamental of $NH_4^+$ or $NH_4^+(NH_3)_4$. The weaker absorption centered at 2900 $cm^{-1}$, and first observed for $n = 7$ at 2870 $cm^{-1}$, is probably a combination band of the $\nu_3$ mode with the stretching mode of the hydrogen bonds between core and 1° ammonias. The peak at 3050 $cm^{-1}$ is assigned to the bending overtone of the core, $2\nu_4$.

The major difference in the spectra of $n = 9$ and 10 in the 2600–3200-$cm^{-1}$ region from that of $n = 8$ lies in the slight blue shift of the intense band at 2820 $cm^{-1}$ for $n = 8$. It appears at 2829 and 2841 $cm^{-1}$ in the $n = 9$ and 10 spectra, respectively. The frequencies of other bands have converged more quickly.

Intensities and positions of peaks in the 3200–3500-$cm^{-1}$ region differ only slightly from the $n = 6$ spectrum with the notable exception of the internal rotation structure, which is absent. The 3220-$cm^{-1}$ peak (D in Figure 9f) is assigned primarily to $^{4}1°$ $N\text{-}H_{astr}^{bd}$, with perhaps contributions from $2\nu_4$ of 2° $NH_3$. We believe the 3320-$cm^{-1}$ peak to be $\nu_1$ of 2° $NH_3$, with the weak shoulder at 3300 $cm^{-1}$ attributed to the symmetric stretch of the two equivalent N–H bonds of the 1° $NH_3$ subunits. The peak at 3380 $cm^{-1}$ (E in Figure 9f) is easily assigned to the antisymmetric stretch of the two equivalent N–H bonds of the 1° subunits bound by 2° $NH_3$'s.

The appearance of the band that peaks at 3415 $cm^{-1}$ is very different from that of the smaller clusters in the same region. The structure observed for $n = 7$ was similarly weak and began to appear a bit broadened, but sharp structure from internal rotation of the 1° $NH_3$'s was still apparent. The corresponding band for $n = 8$ shown in Figure 6g is unmistakably broadened, shifted slightly to the red, and no structure due to internal rotation is evident. (Due to the weak signal for this cluster, a larger wavelength increment between data points and longer averaging time at each point was used for this trace. Spectral resolution is slightly larger than 1 $cm^{-1}$ but is still well inside the expected 12-$cm^{-1}$ structure for internal rotation.)

It appears that this feature is actually the $\nu_3$ band of 2° $NH_3$. Evidently, the 2° subunits are not able to propeller in the same manner as the 1° $NH_3$'s. The latter suggestion is supported, as the loss of structure and a red shift of about 6 $cm^{-1}$ would be expected for $NH_3$ subunits with a relatively high barrier to internal rotation. It is quite possible that the 2° $NH_3$'s do not attach via a linear hydrogen bond, thereby resulting in an orientation not along the 2° $NH_3$'s local $C_3$ axis. It is known from microwave spectroscopy that the neutral ammonia dimer is not held together by a hydrogen bond.[54] If something similar is happening in these large clusters, a larger barrier to internal rotation could result. Cross-linking between 2° subunits would also explain the loss of internal rotation structure.

Another explanation for a higher internal rotation barrier of 2° $NH_3$ as compared to unbound 1° $NH_3$ is related to the low symmetry of 1° $NH_3$ compared to the $NH_4^+$ core. When a 2° $NH_3$ attaches to 1° $NH_3$ with its $C_3$ axis coincident with an NH bond vector of the 1° subunit, that 1° subunit has only two equivalent N–H bonds. The potential function for internal rotation of 2° subunits therefore seems likely to be more complicated, with perhaps a somewhat higher barrier. In any case, there seems to be no doubt that the dominant structure involves four 1° $NH_3$ ligands and four 2° ligands, each attached to a different 1° subunit. Our preferred structure for the $NH_4^+(NH_3)_8$ complex is that shown in Figure 10c.

## Summary and Conclusions

The infrared vibrational predissociation spectra of the ammoniated ammonium ions contain two main classes of spectral features: those that can be assigned to motions of the $NH_4^+$ ion core of the cluster and those that can be attributed to the $NH_3$ solvent molecules. The core vibrations observed can be easily understood in terms of the $\nu_3$ (antisymmetric stretch), $\nu_1$ (symmetric stretch), and $2\nu_4$ (degenerate bending) modes of the $NH_4^+$ ion in several cases, with the application of distorted tetrahedron theory. The most prominent solvent vibrations that are observed are assigned to transitions arising from the first solvent shell (1°) ammonias; transitions of second shell (2°) subunits account for relatively weak features appearing only in the spectra of the largest clusters. For the 1° $NH_3$ molecules not perturbed by second solvation shell (2°) $NH_3$'s, the strongest transitions assigned are analogous to $\nu_3$ (the doubly degenerate antisymmetric stretch) and $2\nu_4$ (the bending mode) of $NH_3$. For the $\nu_3$ type mode, rotational structure is observed on the vibrational transition that has been assigned to an internal rotation of the ammonias about their local $C_3$ axes. The internal rotation structure is observed as a consequence of the selection rule $\Delta K = \pm 1$ for this perpendicular band (perpendicular with respect to the $C_3$ axis of the $NH_3$ subunit whose $\nu_3$ vibration is excited), where $K$ is the quantum number for angular momentum about the $NH_3$ $C_3$ axis. Such a structure is also expected for the $\nu_4$ fundamental, but not for the $\nu_1$ or $\nu_2$ modes.

Trends in the measured vibrational frequencies are observed for both core and solvent vibrations in the $NH_4^+(NH_3)_n$ species

(54) Nelson, Jr., D. D.; Fraser, G. T.; Klemperer, W. *J. Chem. Phys.* **1985**, *83*, 6201.

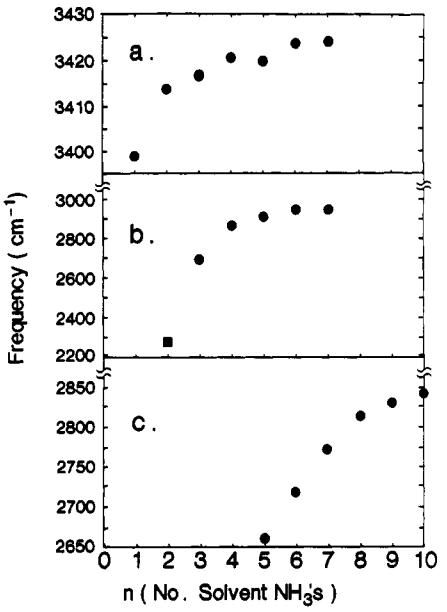


**Figure 11.** (a) Plot of the $^RQ_0$ bands for the internal rotation structure associated with the 1° $NH_3$'s antisymmetric stretching transition as a function of cluster size. (b) Plot of the peak intensity of the antisymmetric stretching band for the ammonium ion core bound only to 1° $NH_3$ molecules as a function of cluster size. The series shows eventual convergence as $n$ increases. See text for discussion. (c) Plot of the peak intensity of the antisymmetric stretching band for the ammonium ion core bound to both 1° and 2° $NH_3$ molecules as a function of cluster size. Converged values are similar to those observed for solutions of ammonium salts dissolved in liquid ammonia. See text for discussion.

which converge at large $n$. The $\nu_3$ antisymmetric stretching vibration for the 1° solvent molecules was first observed in the $n$ = 1 cluster. With $^RQ_0$ centered at 3398.4 $cm^{-1}$, this feature shifts further to the blue and decreases in relative intensity with increasing cluster size. The frequencies of the central $^RQ_0(K=0)$ bands measured for this transition are plotted as a function of cluster size in Figure 11a. The band origins in each case lie about 6 $cm^{-1}$ to the red of the listed frequency. The band origin of free $NH_3$ in the gas phase is 3444 $cm^{-1}$ (see Table I, ref e). It can be seen that, as in the case of other cluster ions observed previously, such as the hydrogen cluster ions, $H_n^+$, and the hydrated hydronium ions, the converged value of this solvent transition lies significantly below the value for the free molecule due to the red shift imposed by the solvation interaction even at large distances from the ion core.

A similar plot for the frequencies of the antisymmetric stretching vibration of the core bound to only 1° $NH_3$'s is shown in Figure 11b. The first point in the plot for the $n$ = 2 cluster is from Schwarz's measurement which he tentatively assigned to the component of the antisymmetric stretch of the $NH_4^+$ ion bound by two $NH_3$'s. We observe the analogous feature in the $n$ = 3–7 spectra shift to the blue and decrease in relative intensity, converging by the $n$ = 7 spectrum to 2989 $cm^{-1}$. The frequencies for similar core stretching vibrations with an attached 2° $NH_3$ as well are plotted in Figure 11c.

The spectra have clearly indicated, in agreement with previous thermochemical measurements and theoretical calculations, that a well-defined shell structure exists. The first solvent shell is completed by four ligands. The fifth ligand hydrogen-bonds to a 1° $NH_3$, with only one N–H bond of the 1° subunit directly affected. Successive ammonia ligands hydrogen-bond to other 1° subunits in the same way until the $n$ = 8 complex shown in Figure 10c is obtained. In this complex each 1° subunit is bound by one 2° subunit.

In the complexes $n$ = 1–7, any 1° $NH_3$ that is not bonded to a 2° subunit has a $\nu_3$ band which exhibits the structure characteristic of nearly free internal rotation of that 1° subunit. A 1° $NH_3$ that *is* bonded to a 2° subunit might well undergo internal rotation, but the characteristic spacing of the Q branches in the associated $\nu_3$ band will be less than the 1-$cm^{-1}$ laser line width employed for these studies. For the 2° $NH_3$, the barrier to internal rotation about the local $C_{3v}$ axes evidently is higher, or the transition fails to carry sufficient oscillator strength to be observed, as the spectrum of the $n$ = 8 cluster indicates no such structure.

For the $n$ = 9 and 10 complexes, it is not yet clear what binding sites(s) the outermost ligands occupy. If they attach to 2° $NH_3$ subunits, one would expect a new band to appear, red-shifted by perhaps 100 wavenumbers from the core $\nu_3$ stretch at ≈2830 $cm^{-1}$. This is not observed. It may be that the 9th and 10th ligands attach loosely to 1° $NH_3$ subunits. Therefore, although we believe that some sort of shell structure is completed at $n$ = 8 ($NH_4^+(NH_3)_8$), this structure is not so well-defined as that filled at $n$ = 4. We could, for example, say that the 9th and 10th ligands enter the 2′ shell rather than 3; the second shell might be 1/3 or 1/2 full when it contains four ligands. In any case, it is useful to note that the convergence plot of Figure 11c seems to show a slight kink at $n$ = 8, with such small frequency shifts for $n$ = 9, 10 that the binding of these ligands is apparently quite weak.

The spectra that were obtained for $n$ = 9–10 are quite similar to that of $n$ = 8, indicating that the $NH_4^+$ core, at least, is affected only slightly in its infrared absorption properties by the addition of these ligands. Of course, there may be other properties of the core or of the rest of the complex that are more significantly affected. The infrared probe is sensitive to bond length and bond strength, and we can say that these characteristics of the $NH_4^+$ core are no longer changing. It is probable that these properties are likely to show significant discontinuities for certain larger values of $n$, if special structures form.

A comparison of the spectra of ammonium salts with weakly interacting counter ions such as $NO_3^-$ or $ClO_4^-$ in ammonia solution with that of the $n$ = 8 ionic cluster shows unmistakable similarity, particularly at low temperatures. For the more strongly interacting counterion $Cl^-$, the spectrum is still very similar, especially for a mole ratio $NH_3$:$ClNH_4$ ≥ 6 (see fig. 2 of ref 3). In general, the broad, intense absorption in the 2800-$cm^{-1}$ region of ammonium salts should be associated with a $\nu_3$ type vibration of solvated $NH_4^+$. In the 3200–3500-$cm^{-1}$ region, the spectrum is quite similar to that of liquid ammonia[52] or neutral ammonia clusters $(NH_3)_n$ ($n$ = 3–5).[53] So far as the infrared spectra are concerned, the $n$ = 8 complex is already quite close to an $NH_4^+$ in a liquidlike environment. In other words, the very strong "chemicallike" bonding of the $NH_4^+$ to the solvent molecules gets diluted over the large number of subunits by $n$ = 8 so that the interaction of the ionic core with additional $NH_3$'s is comparable to that between neutral $NH_3$'s.

While the spectra of crystalline ammonium salts have been well-understood for many years, that of the same salts in $NH_3$ solution has been more difficult to interpret. The liquid-phase vibrational bands tend to be very broad, even when compared to those of the solid phase, and the relative intensities of the bands can vary dramatically with the chemical conditions. The spectra of cold ammoniated ammonium clusters in the gas phase can therefore contribute a great deal to our understanding of the interactions present in such solutions.

*Acknowledgment.* This work was supported by the Director, Office of Energy Research, Office of Basic Energy Sciences, Chemical Sciences Division, under Contract DE-AC03-76SF00098.

**Registry No.** $NH_4^+$, 14798-03-9; $NH_3$, 7664-41-7.